Anisotropic flow fluctuations in Pb+Pb collisions at LHC

L. Bravina

in collaboration with

H.Brusheim Johansson, J.Crkovska, G.Eyyubova, E.Fotina, V.Korotkikh, I.Lokhtin, L.Malinina, E.Nasarova, S.Petrushanko, A.Snigirev, E.Zabrodin

International Conference on New Frontiers in Physics ICNFP-2015

Kolymbari, Crete, Greece, 23-29.08.2015

Phase diagram

SIS	2 AGeV	(FOPI, TAPS, HADES)
AGS	10 AGeV	(E896, E917, E910)
SPS	30-160 AGeV	(NA49, NA50, NA60, WA98…)
RHIC	7-200 GeV	(BRAHMS, PHENIX, PHAR[illegible]IX, PHOBOS, STAR)
LHC	2.76-5.1 TeV	(ALICE, CMS, ATLAS)
FAIR	30 AGeV	(CBM)
NICA	10 GeV	(MPD, SPD)

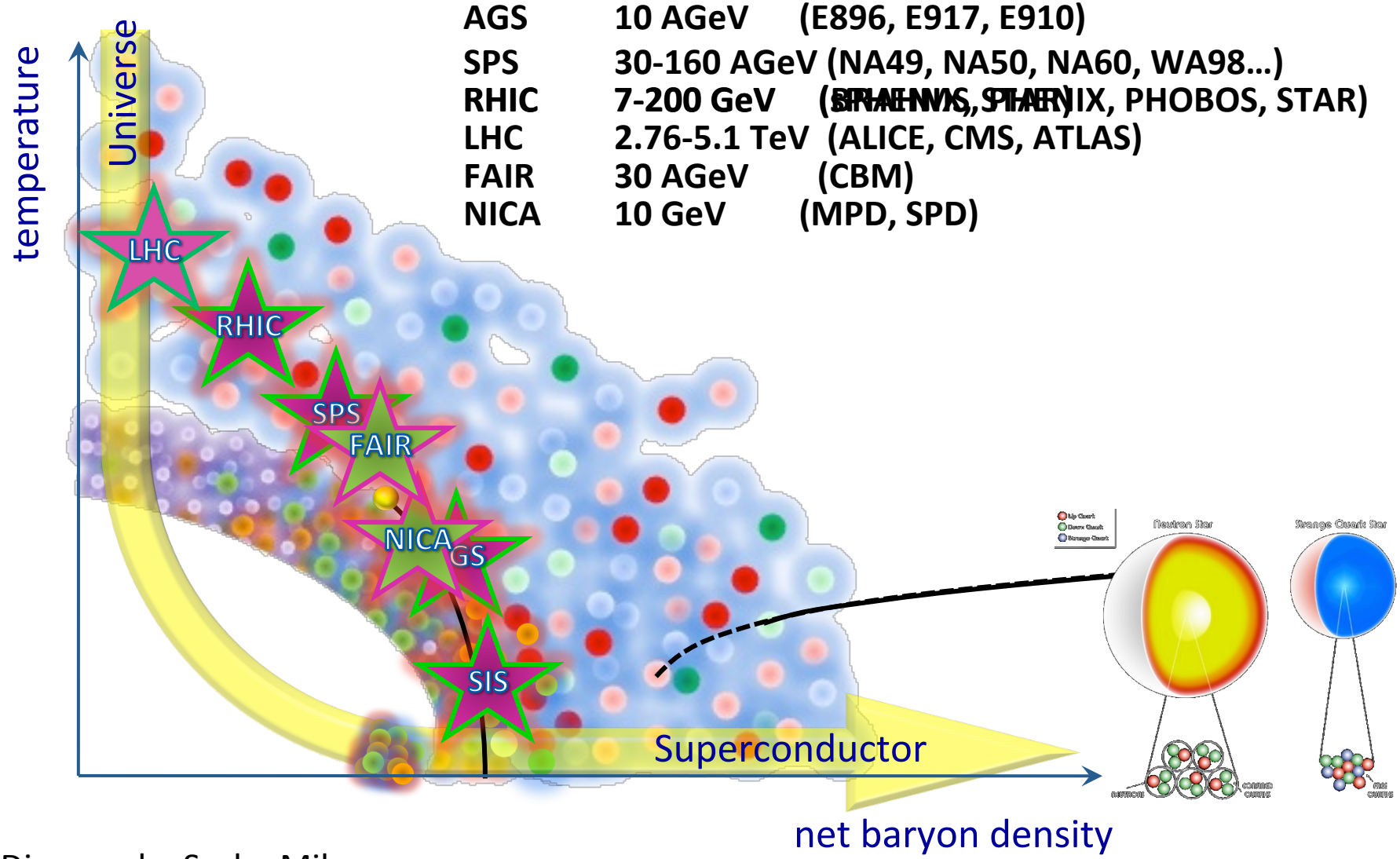

Diagram by Sasha Milov

Dynamic Regimes

Parton distribution,
Nuclear geometry
Nuclear shadowing

Parton production &
regeneration
(or, sQGP)

Chemical freeze-out
(Quark recombination)

Jet fragmentation
functions

Hadron rescattering

Thermal freeze-out

Hadron decays

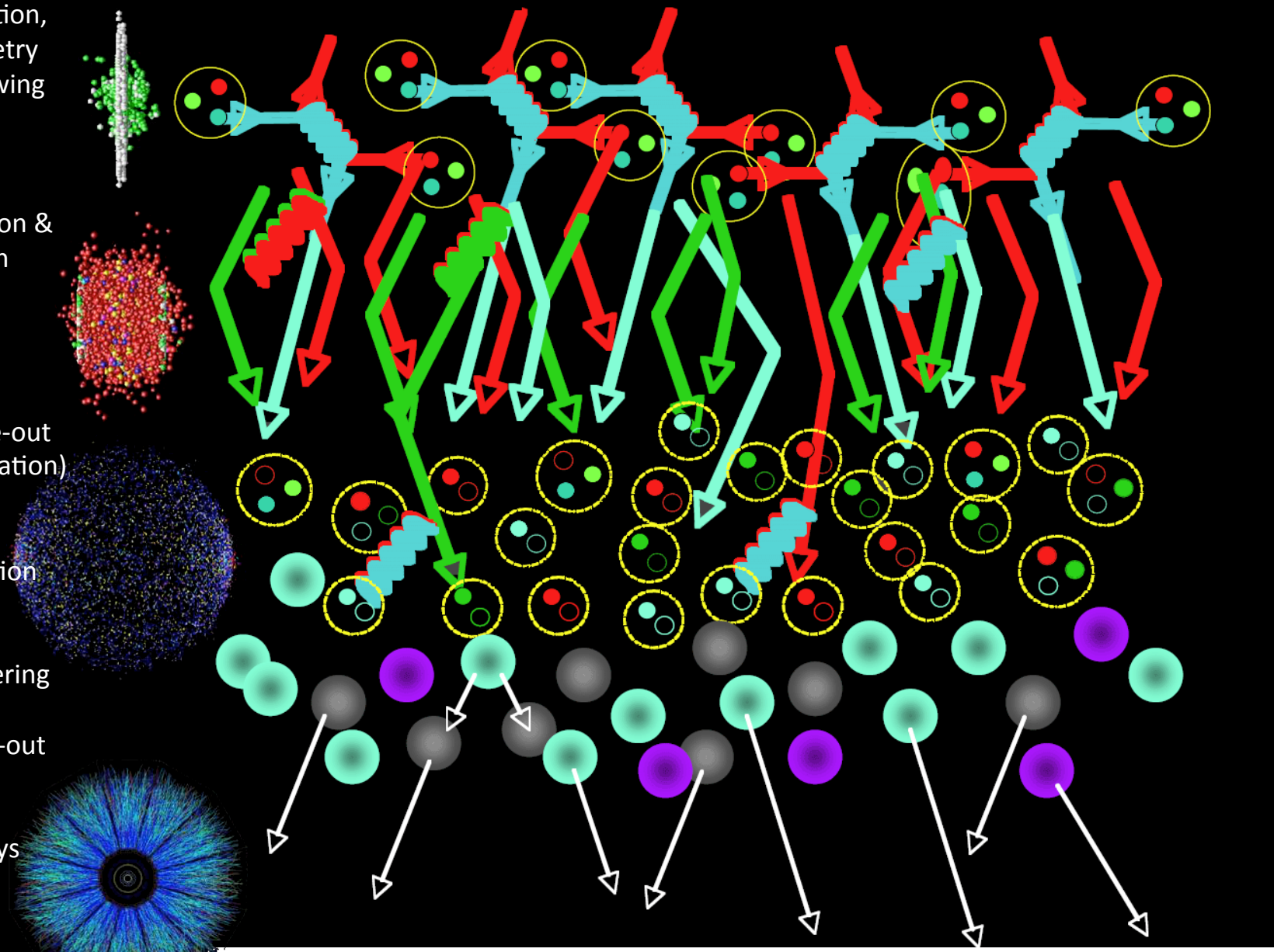

Diagram by Peter Steinberg

ELLIPTIC FLOW

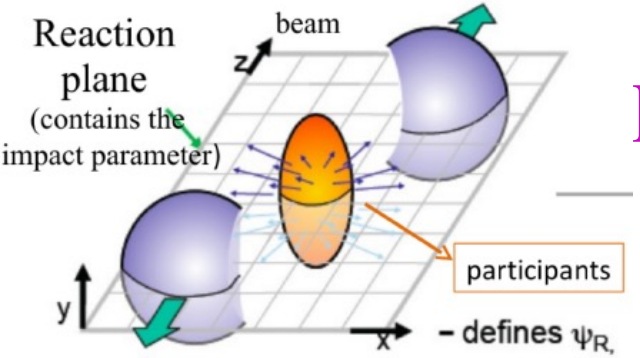

Initial spatial anisotropy is converted to anisotropy in momentum space

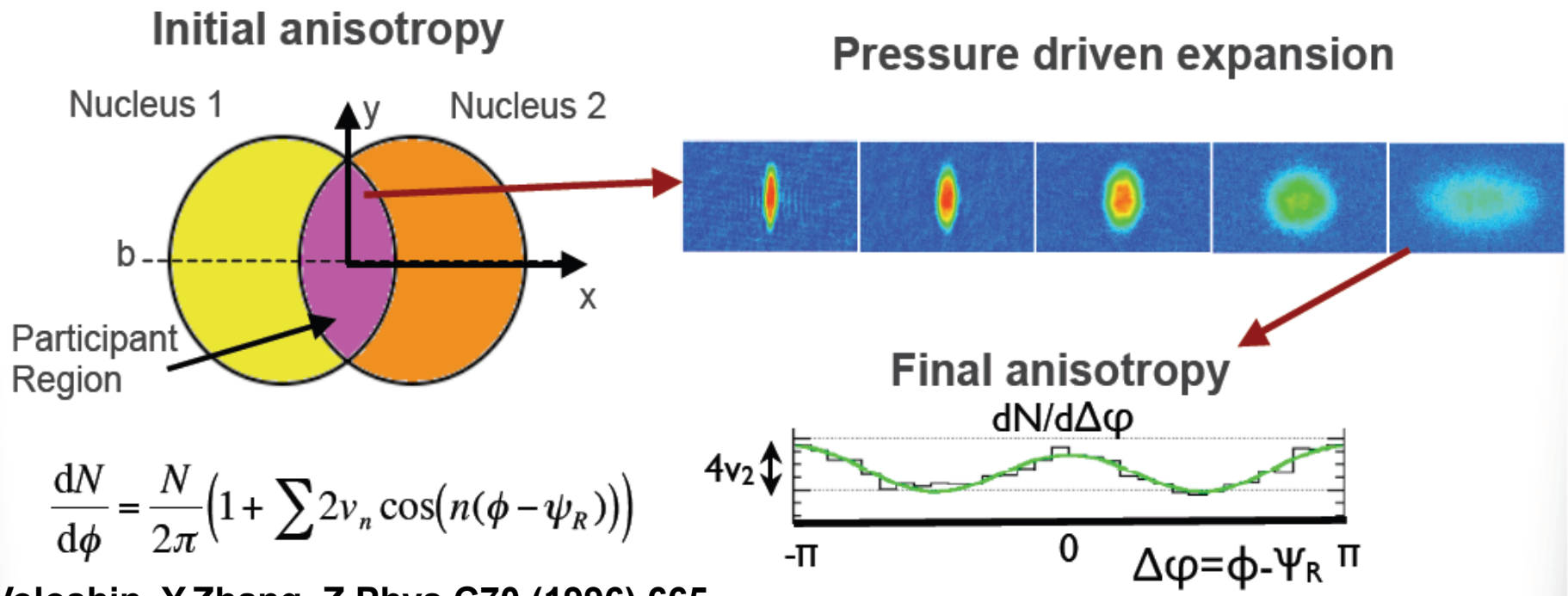

$$\frac{dN}{d\phi} = \frac{N}{2\pi}\left(1 + \sum 2v_n \cos\left(n(\phi - \psi_R)\right)\right)$$

S.Voloshin, Y.Zhang, Z.Phys.C70 (1996) 665

$$v_2 = \left\langle \cos\left(2(\phi - \underline{\psi_R})\right)\right\rangle \propto \varepsilon$$

Elliptic flow is quantified by the second Fourier coefficient (v_2) of the observed particle distribution

ECCENTRICITY

STANDARD

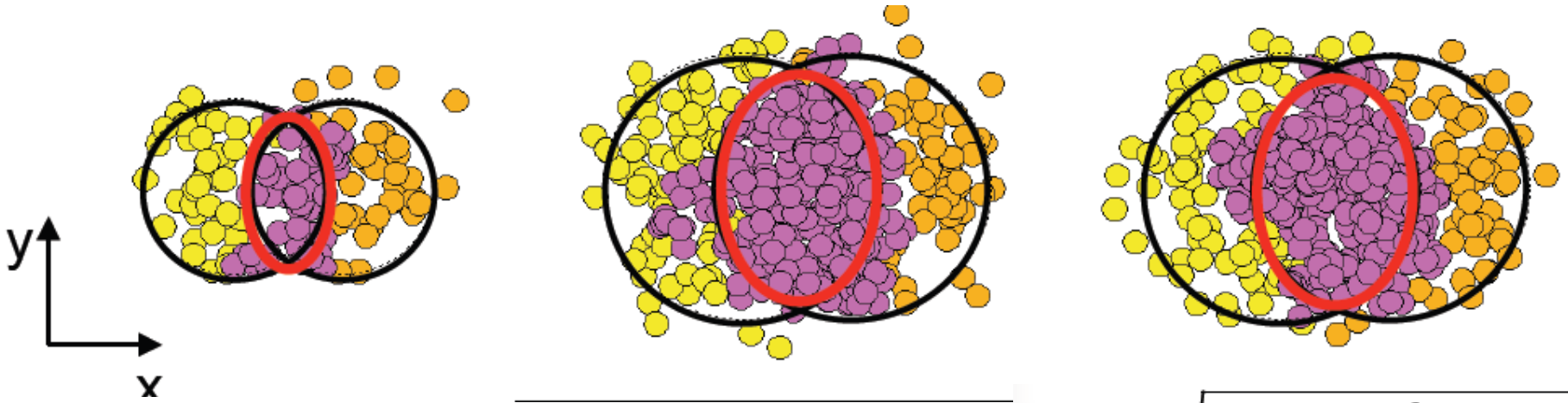

$$\varepsilon_{\mathbf{RP}} = \frac{\langle y^2 \rangle - \langle x^2 \rangle}{\langle y^2 \rangle + \langle x^2 \rangle}$$

PARTICIPANT

$$\varepsilon_{\mathbf{part}} = \frac{\sqrt{\left(\sigma_y^2 - \sigma_x^2\right)^2 + 4\sigma_{xy}^2}}{\sigma_y^2 + \sigma_x^2}$$

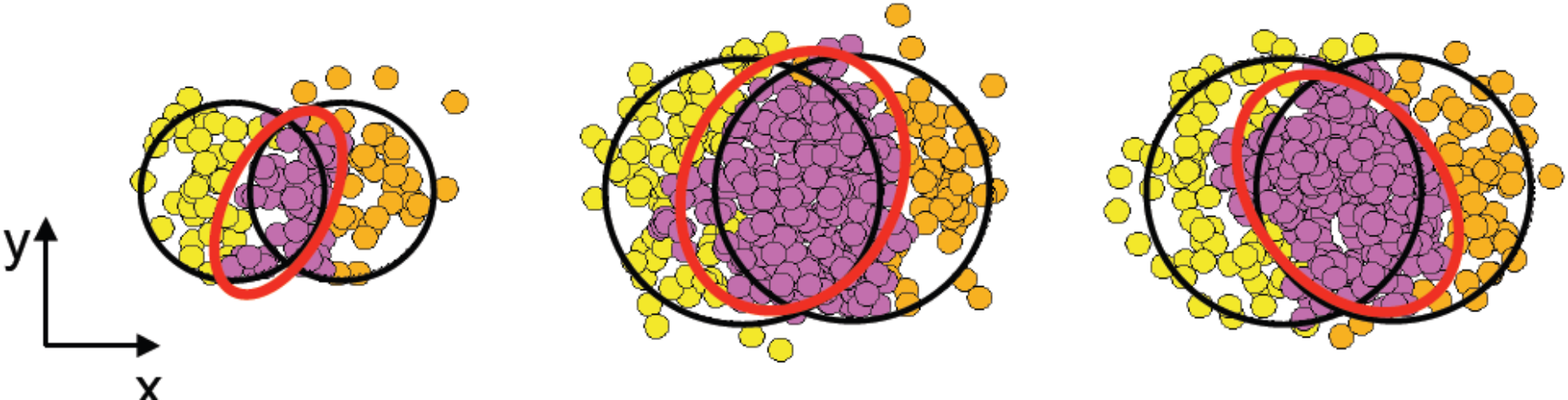

TRIANGULAR FLOW

B. Alver and G.Roland, PRC 81 (2010) 054905

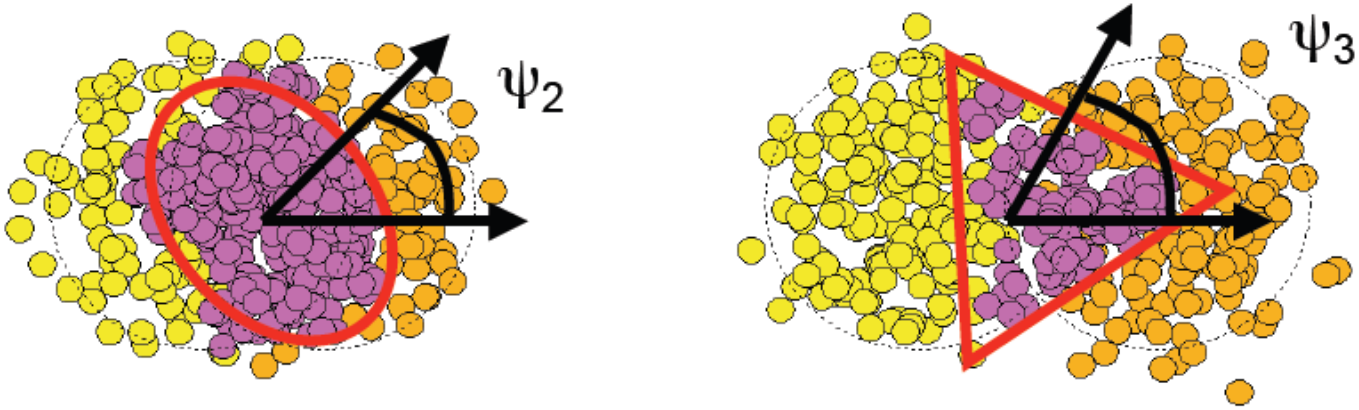

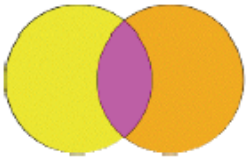

$$\frac{dN}{d\phi} = \frac{N}{2\pi}\left(1 + \sum 2v_n \cos\left(n(\phi - \psi_R)\right)\right)$$

$$v_2 = \left\langle \cos\left(2(\phi - \psi_R)\right)\right\rangle$$

$$v_3 = 0$$

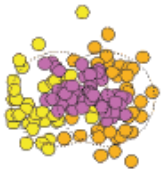

$$\frac{dN}{d\phi} = \frac{N}{2\pi}\left(1 + \sum 2v_n \cos\left(n(\phi - \psi_n)\right)\right)$$

$$v_2 = \left\langle \cos\left(2(\phi - \psi_2)\right)\right\rangle$$

$$v_3 = \left\langle \cos\left(3(\phi - \psi_3)\right)\right\rangle$$

The triangular initial shape leads to triangular hydrodynamic flow

CROSS-TALK BETWEEN FLOW HARMONICS

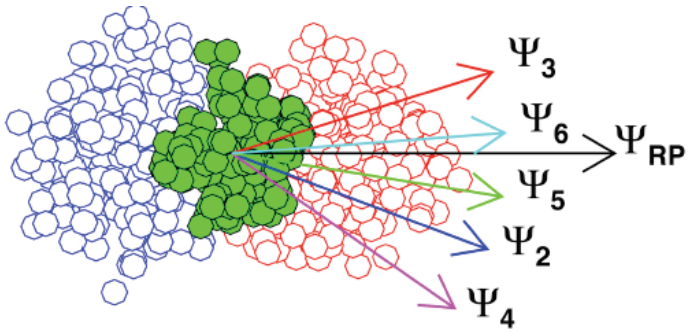

ψ_n: participant plane

G.-Y. Qin et al, PRC 82 (2010) 064903

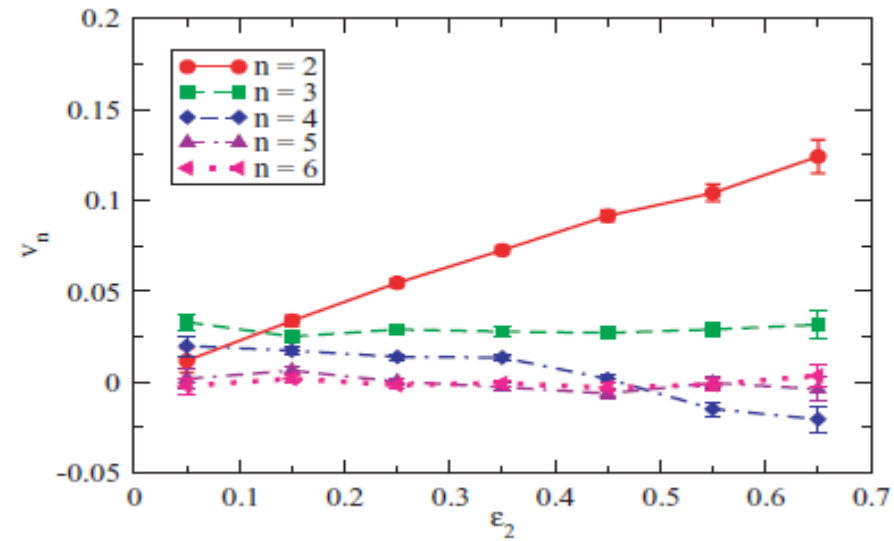

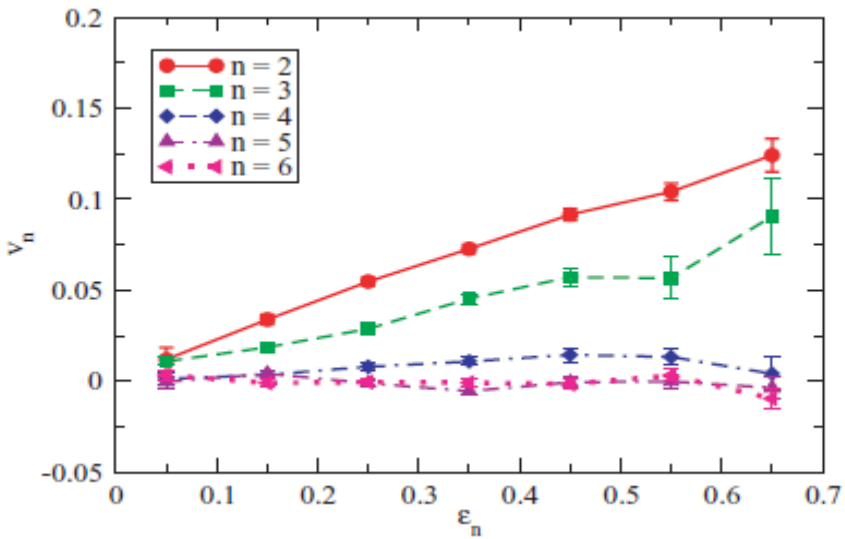

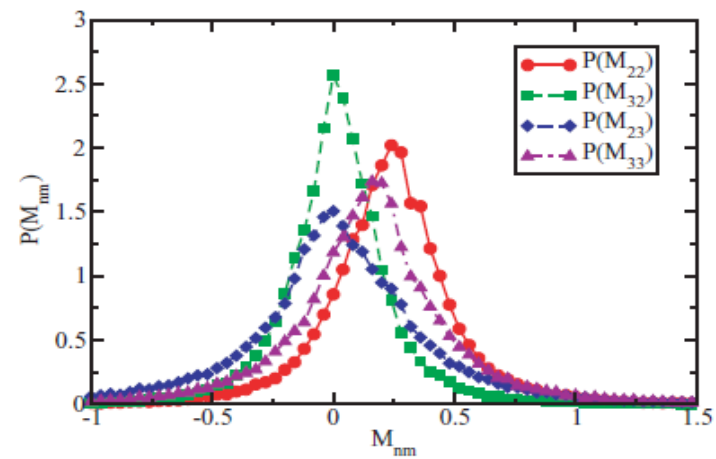

$$\begin{pmatrix} v_2 \\ v_3 \end{pmatrix} = \begin{pmatrix} M_{22} & M_{23} \\ M_{32} & M_{33} \end{pmatrix} \begin{pmatrix} \epsilon_2 \\ \epsilon_3 \end{pmatrix}$$

Only the first few flow harmonics of final-state hadrons survive after hydrodynamic evolution

CROSS-TALK BETWEEN FLOW HARMONICS

Z. Qiu and U. Heinz, PRC 84 (2011) 024911

$$\varepsilon_n e^{in\psi_n^{\mathrm{PP}}} = -\frac{\int dx\, dy\, r^2 e^{in\phi}\, e(x,y)}{\int dx\, dy\, r^2\, e(x,y)}$$

$$v_n(y, p_T)\, e^{in\psi_n^{\mathrm{EP}}(y,p_T)} = \frac{\int d\phi_p\, e^{in\phi_p} \frac{dN}{dy\, p_T dp_T\, d\phi_p}}{\frac{dN}{dy\, p_T dp_T}}$$

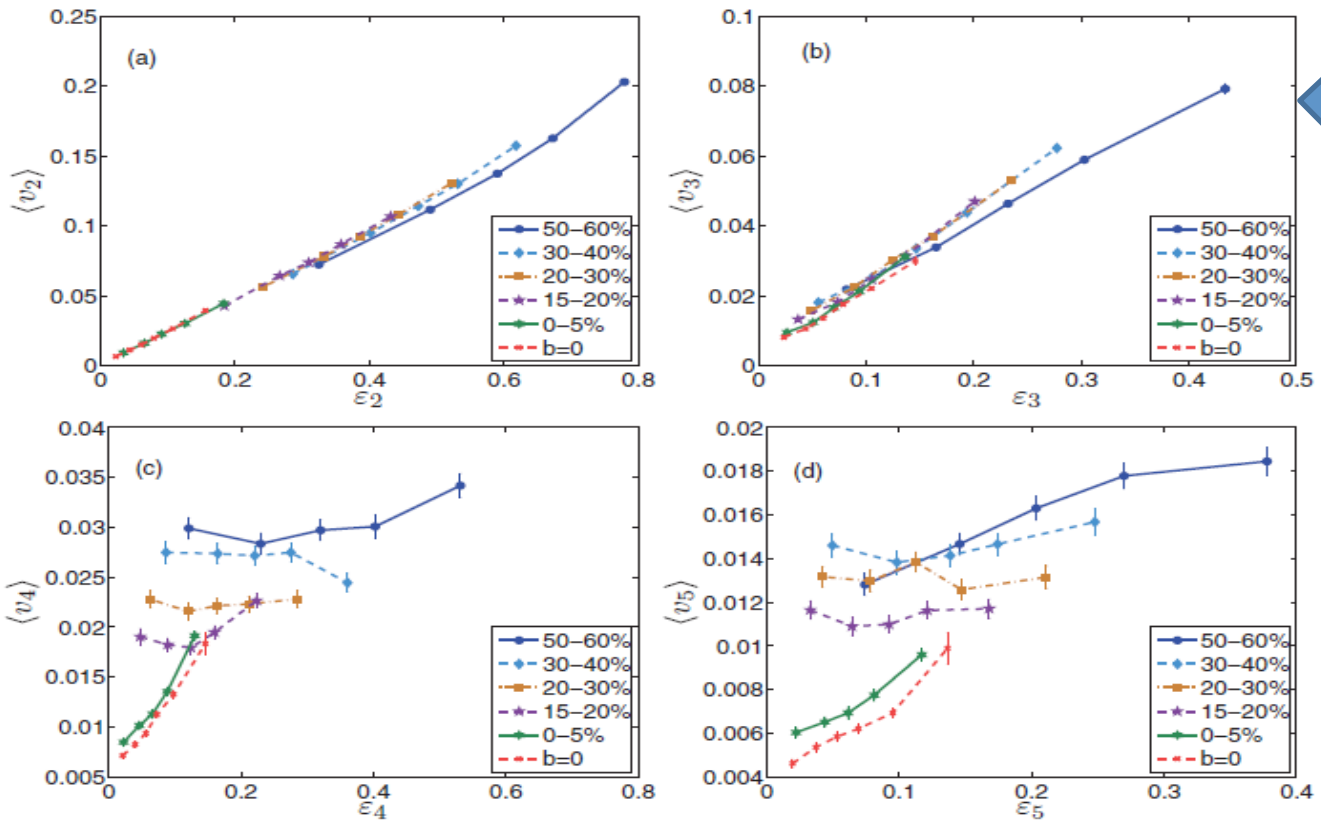

(1) The basic response of v_2 and v_3 to eccentricities is approx. linear

(2) Higher flow coefficients show poor correlation with the eccentricities of the same order

II. HYDJET++ = FASTMC + PYQUEN

HYDJET++ (soft): hydrodynamics with resonances

Soft (hydro) part of HYDJET++ is based on the adapted FAST MC model:
Part I: N.S.Amelin, R.Lednisky, T.A.Pocheptsov, I.P.Lokhtin, L.V.Malinina, A.M.Snigirev, Yu.A.Karpenko, Yu.M.Sinyukov, Phys. Rev. C 74 (2006) 064901
Part II: N.S.Amelin, R.Lednisky, I.P.Lokhtin, L.V.Malinina, A.M.Snigirev, Yu.A.Karpenko, Yu.M.Sinyukov, I.C.Arsene, L.Bravina, Phys. Rev. C 77 (2008) 014903

- fast HYDJET-inspired MC procedure for soft hadron generation multiplicities are determined assuming thermal equilibrium
- hadrons are produced on the hypersurface represented by a parameterization of relativistic hydrodynamics with given freeze-out conditions
- chemical and kinetic freeze-outs are separated
- decays of hadronic resonances are taken into account (360 particles from SHARE data table) with severely modified decayer
- written within ROOT framework (C++)
- contains 16 free parameters (but this number may be reduced to 9)

See talks by G. Eyyubova (plenary) and B.H. Brushein Johansson (parallel) (26.08)

Parton rescattering and jet quenching

Collisional loss
(high momentum transfer approximation)

Radiative loss
(BDMS model, coherent radiation)

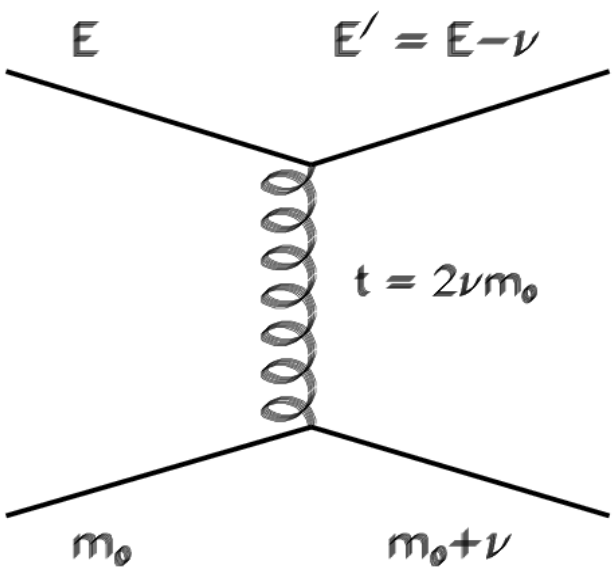

+

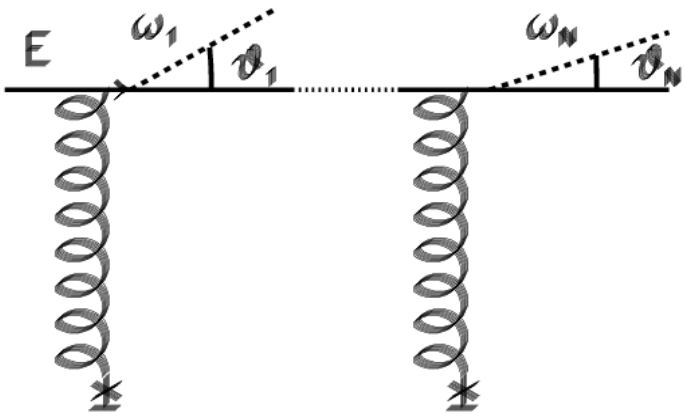

Strength of e-loss in PYQUEN is determined mainly by initial maximal temperature T0 of hot matter in central (b=0) PbPb collisions (depends also on formation time τ_0 and # of quark flavors N_f)

PYQUEN: physics frames

General kinetic integral equation:

$$\Delta E(L,E)=\int_0^L dx\,\frac{dP}{dx}(x)\,\lambda(x)\,\frac{dE}{dx}(x,E),\quad \frac{dP}{dx}(x)=\frac{1}{\lambda(x)}\exp(-x/\lambda(x))$$

1. Collisional loss and elastic scattering cross section:

$$\frac{dE}{dx}=\frac{1}{4T\lambda\sigma}\int_{\mu_D^2}^{t_{max}} dt\,\frac{d\sigma}{dt}\,t,\quad \frac{d\sigma}{dt}\simeq C\frac{2\pi\alpha_s^2(t)}{t^2},\quad \alpha_S=\frac{12\pi}{(33-2N_f)\ln(t/\Lambda_{QCD}^2)},\quad C=9/4(\%gg),1(gq),4/9(qq)$$

2. Radiative loss (BDMS):

$$\frac{dE}{dx}(m_q=0)=\frac{2\alpha_s C_F}{\pi\tau_L}\int_{E_{LPM}\sim\lambda_g\mu_D^2}^{E} d\omega\left[1-y+\frac{y^2}{2}\right]\ln\left|\cos(\omega_1\tau_1)\right|,\quad \omega_1=\sqrt{i\left(1-y+\frac{C_F}{3}y^2\right)\bar{k}\ln\frac{16}{\bar{k}}},\quad \bar{k}=\frac{\mu_D^2\lambda_g}{\omega(1-y)},\quad \tau_1=\frac{\tau_L}{2\lambda_g},\quad y=\frac{\omega}{E},\quad C_F=\frac{4}{3}$$

"dead cone" approximation for massive quarks:

$$\frac{dE}{dx}(m_q\neq 0)=\frac{1}{\left(1+(l\omega)^{3/2}\right)^2}\frac{dE}{dx}(m_q=0),\qquad l=\left(\frac{\lambda}{\mu_D^2}\right)^{1/3}\left(\frac{m_q}{E}\right)^{4/3}$$

III. Triangular and elliptic flows in HYDJET++ : interplay of hydrodynamics and jets

Generation of elliptic and triangular flows

V_2

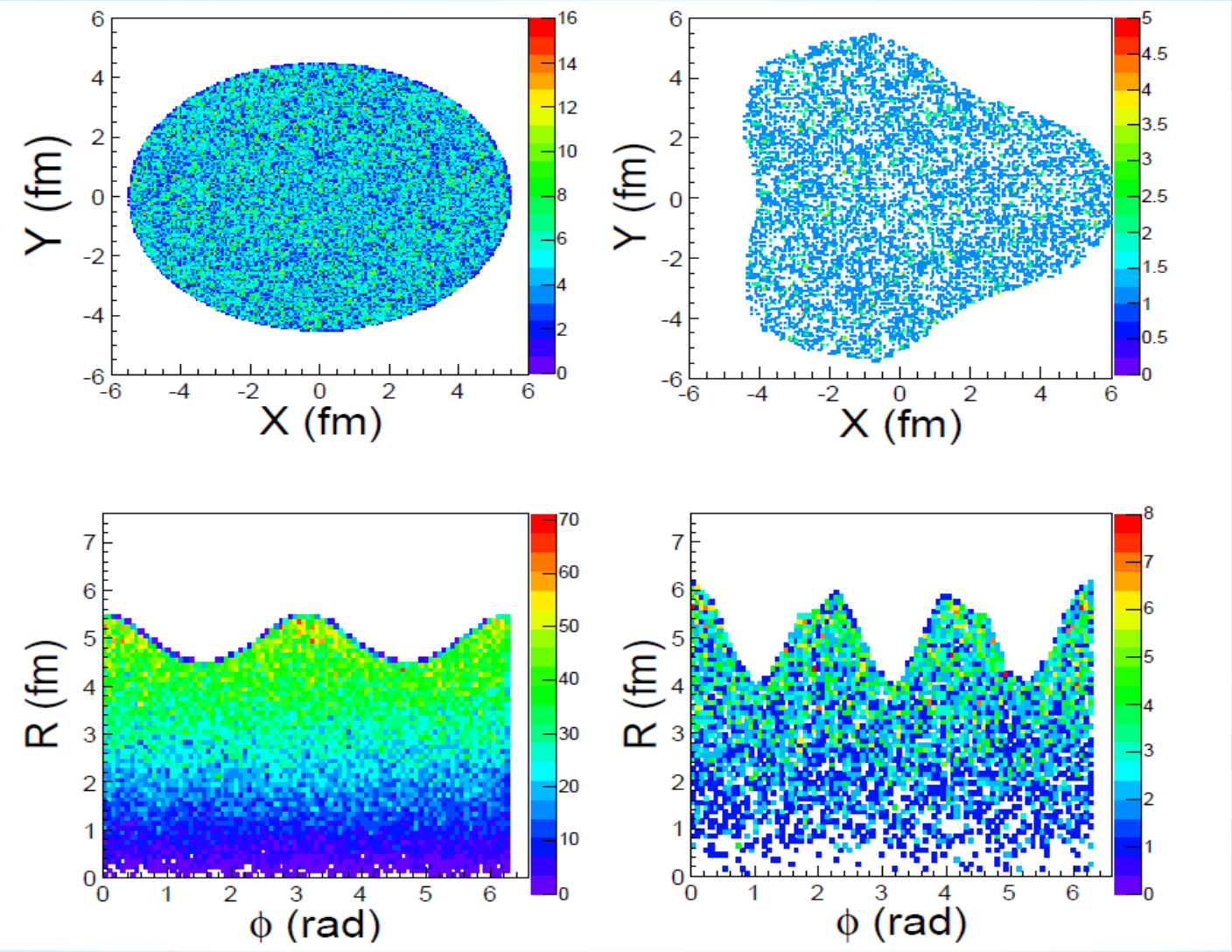

V_3

$$R(b,\phi)=R_s(b)\frac{\sqrt{1-\epsilon^2(b)}}{\sqrt{1+\epsilon(b)\cos(2\phi)}}$$

$$R(b,\varphi) = R_{ell}(b,\varphi)[1+\epsilon_3(b)\cos[3(\varphi-\Psi_3)]]$$

LHC data vs. HYDJET++ model

Elliptic flow

Pb+Pb @ 2.76 ATeV

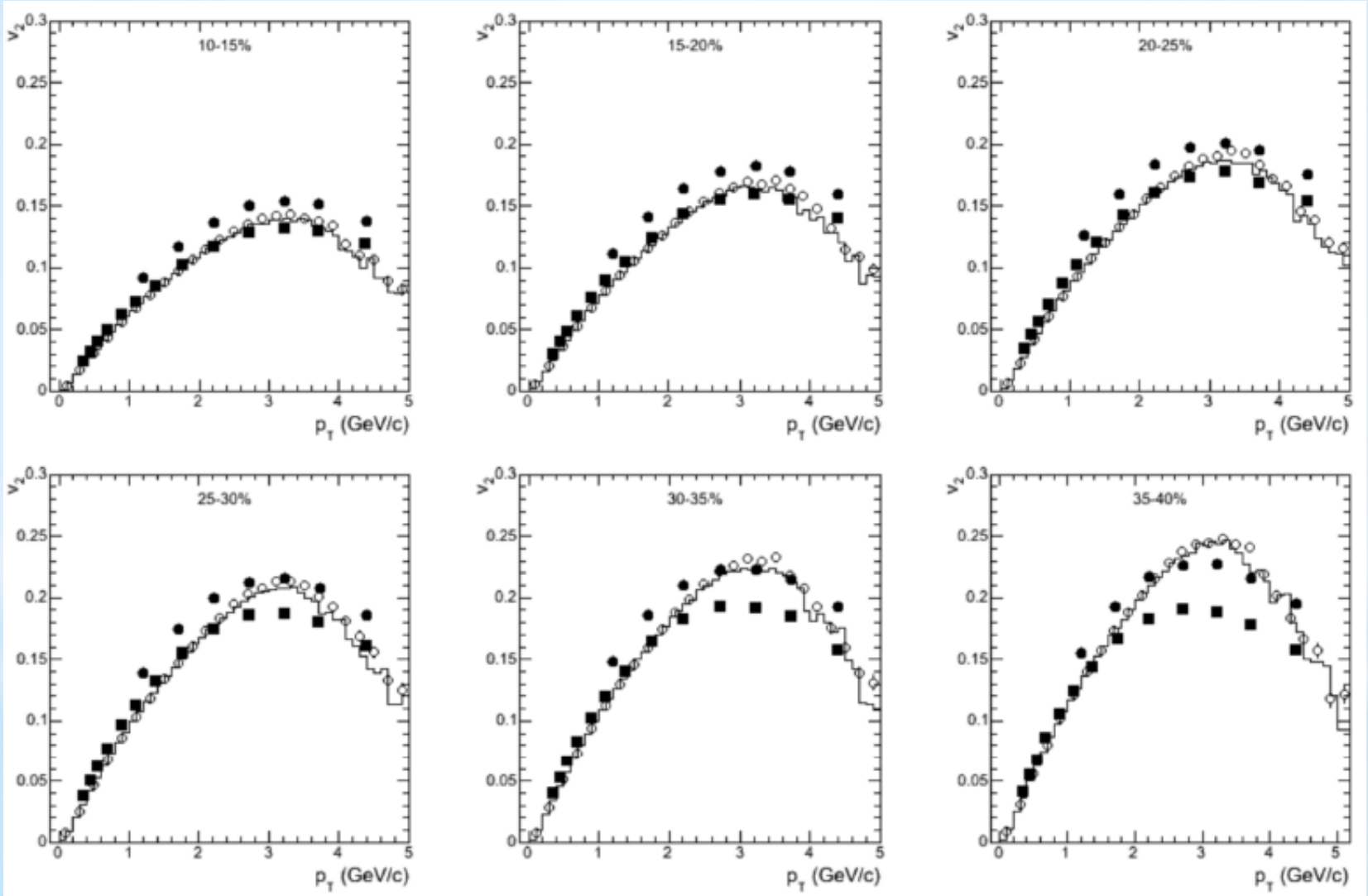

Closed points: CMS data v_2{2Part & LYZ};
Open points and histograms: HYDJET++ v_2{EP & Psi2}

L.B. et al., Eur. Phys. J C74 (2014) 2807

LHC data vs. HYDJET++ model

Triangular flow

Pb+Pb @ 2.76 ATeV

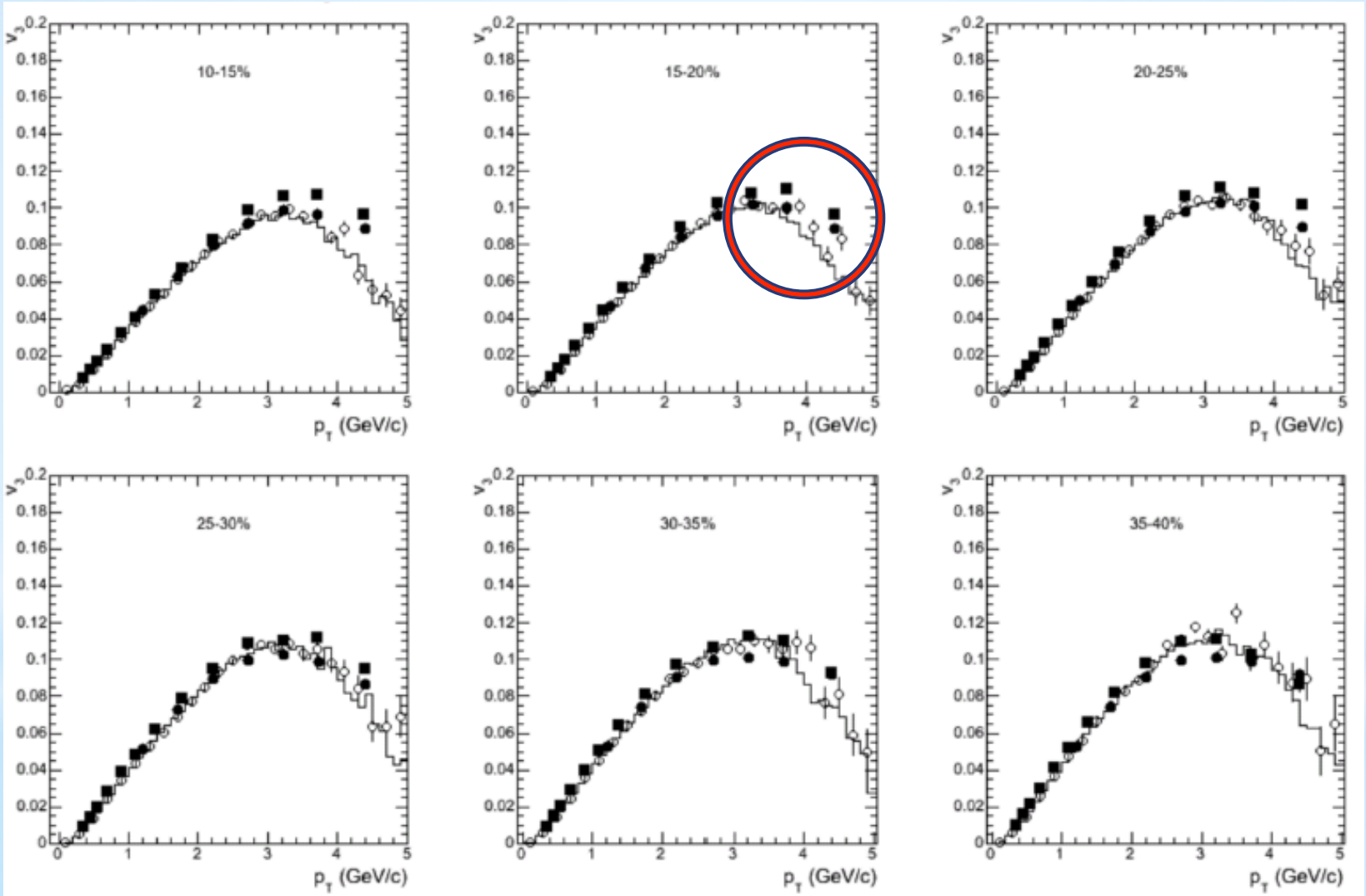

L.B. et al., Eur. Phys. J C74 (2014) 2807

Closed points: CMS data v_3{2Part & LYZ};
Open points and histograms: HYDJET++ v_3{EP & Psi3}

Interplay of hydrodynamics and jets

Triangular flow

Pb+Pb @ 2.76 ATeV

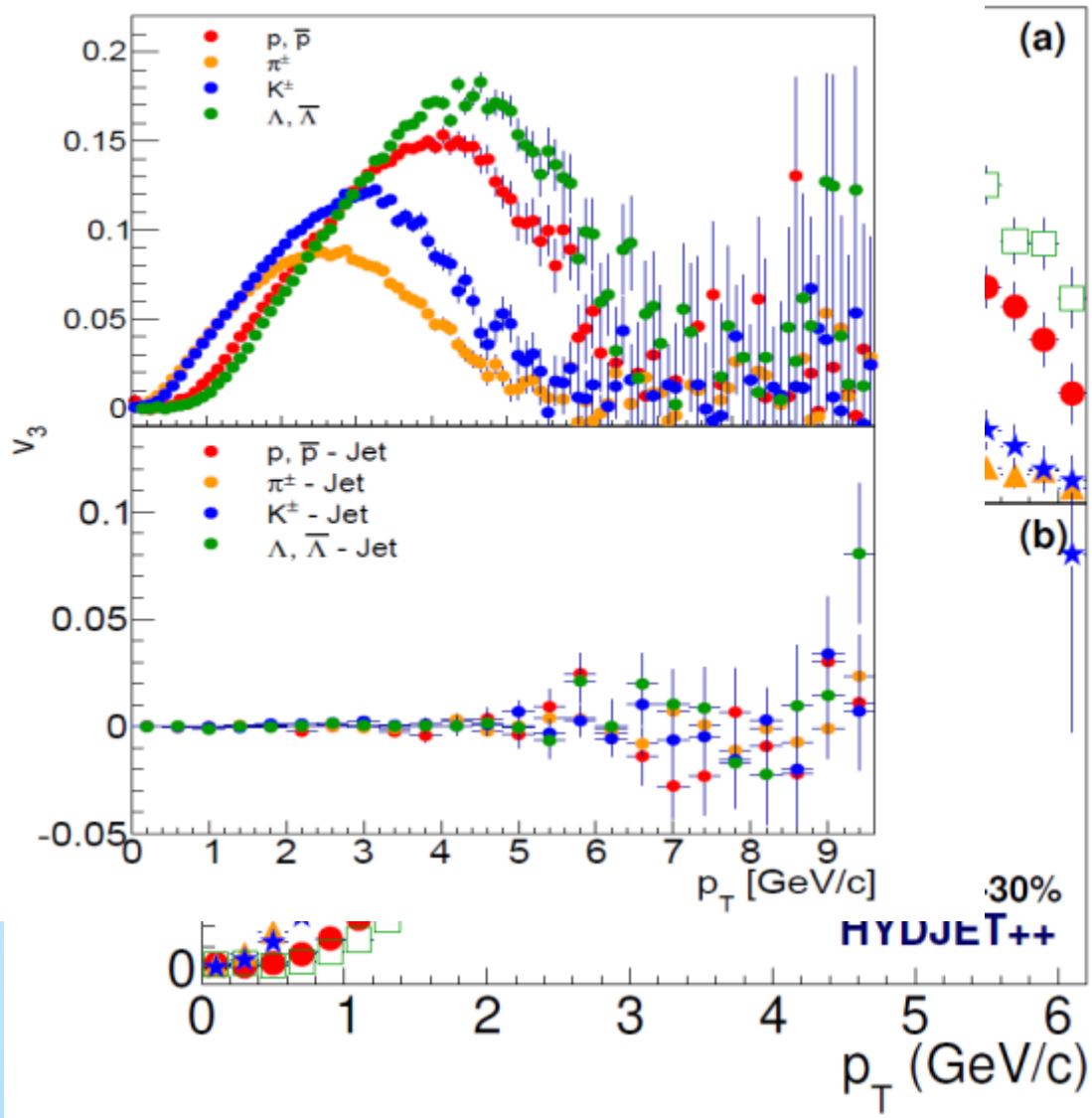

J. Crkovska et al., to be submitted

Hydrodynamics gives **mass ordering** of v_3

The model possesses **crossing** of baryon and meson branches

The reason for the mass ordering break at 2 GeV/c is traced to **hard processes (jets)**

Ridge as interplay of v_2 and v_3

$$\frac{dN^{pairs}}{d\Delta\varphi} \propto 1 + 2\sum_{n=1}^{\infty} V_n(p_T^{tr}, p_T^{a}) \cos n(\Delta\varphi)$$

Angular pair correlations

$$C(\Delta\eta, \Delta\varphi) \equiv \frac{d^2 N^{pair}}{d\Delta\eta d\Delta\varphi}$$

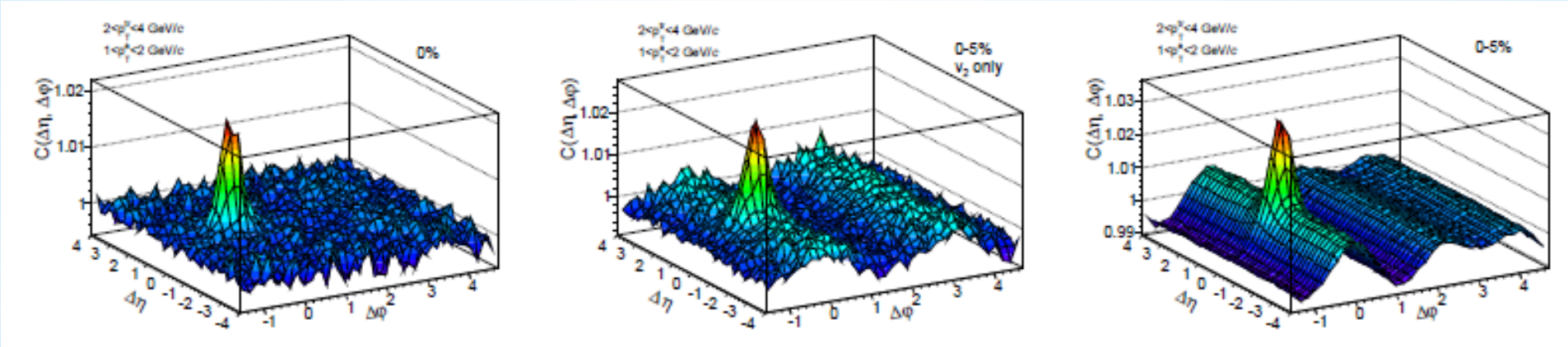

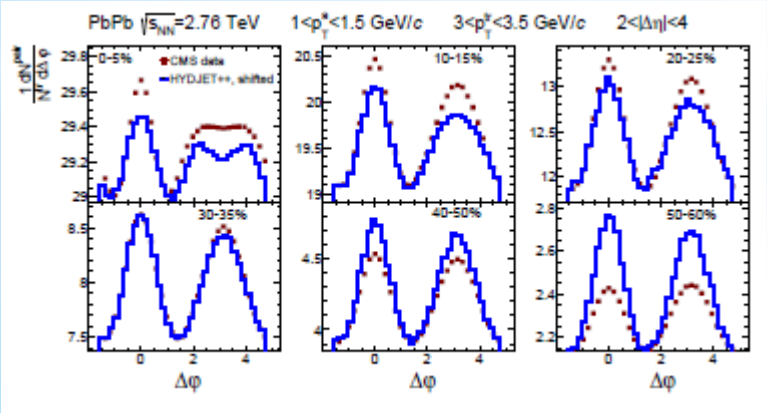

The long-range correlations appear due to flow; v3 is responsible for double-hump structure; the measured amplitude of the ridge at mid-central and semi-peripheral events is well described by a superposition of v2 and v3

G. Eyyubova et al., PRC 91, 064907 (2015)

IV. Anisotropic flow fluctuations

Intrinsic fluctuations in HYDJET++

Event-by-event flow vector V_n

Pb+Pb @ 2.76 ATeV

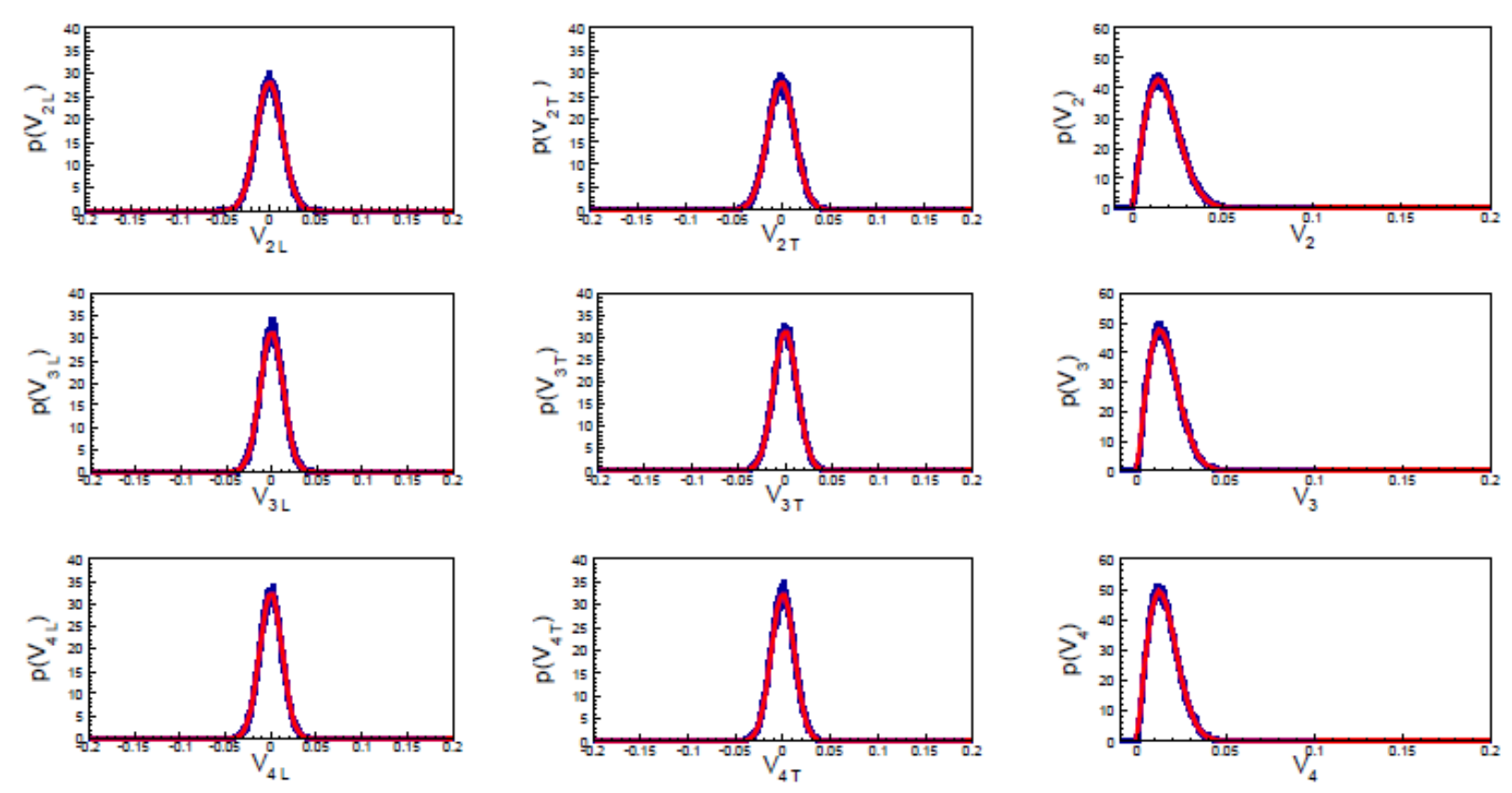

$$p(\boldsymbol{V}_n) = \frac{1}{2\pi\sigma_n^2}\exp[-\boldsymbol{V}_n^2/(2\sigma_n^2)]$$

$$p(V_n) = \frac{V_n}{\sigma_n^2}\exp[-V_n^2/(2\sigma_n^2)]$$

Centrality = 0%, i.e. $\varepsilon = \delta = \varepsilon_3 = 0$

S.Voloshin et al., PLB 659 (2008) 537;
R.Bhalerao, J.-Y. Ollitrault, PLB 641 (2006) 260

L.B. et al., to be submitted

Intrinsic fluctuations in HYDJET++

Event-by-event flow vector V_n

Pb+Pb @ 2.76 ATeV

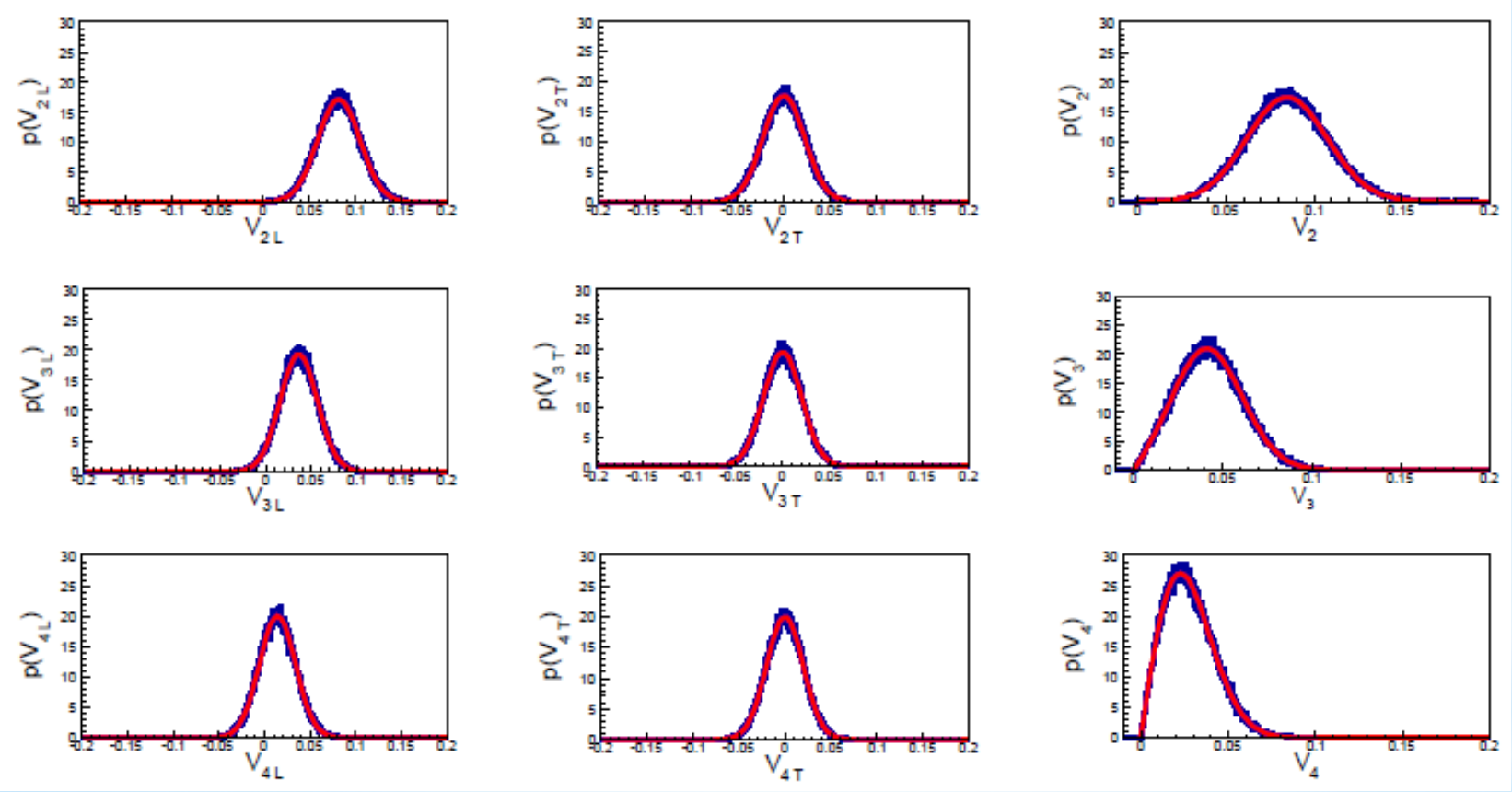

$$p(V_{nL}) = \frac{1}{\sqrt{2\pi\sigma_n^2(b)}} \exp\left[-\frac{(V_{nL} - \langle V_{nL}\rangle)^2}{2\sigma_n^2(b)}\right] \quad p(V_{nT}) = \frac{1}{\sqrt{2\pi\sigma_n^2(b)}} \exp\left[-\frac{(V_{nT})^2}{2\sigma_n^2(b)}\right]$$

Centrality = 20-25%

$$p(V_n) = \frac{V_n}{\sigma_n^2(b)} \exp\left[-\frac{V_n^2 + \langle V_{nL}\rangle^2}{2\sigma_n^2(b)}\right] I_0\left(\frac{V_n\langle V_{nL}\rangle}{\sigma_n^2(b)}\right)$$

S.Voloshin et al., PLB 659 (2008) 537;
R.Bhalerao and J.-Y. Ollitrault, PLB 641 (2006) 260

Bayesian unfolding procedure

$$\frac{dN}{d\varphi} \propto 1 + 2\sum_{n=1}^{\infty} V_{\mathrm{n}}^{\mathrm{obs}} \cos\left[n(\varphi - \Psi_{\mathrm{n}}^{\mathrm{obs}})\right] =$$
$$= 1 + 2\sum_{n=1}^{\infty} (V_{\mathrm{n,x}}^{\mathrm{obs}} \cos n\varphi + V_{\mathrm{n,y}}^{\mathrm{obs}} \sin n\varphi)$$

$$V_{\mathrm{n}}^{\mathrm{obs}} = \sqrt{(V_{\mathrm{n,x}}^{\mathrm{obs}})^2 + (V_{\mathrm{n,y}}^{\mathrm{obs}})^2}\ ,$$
$$V_{\mathrm{n,x}}^{\mathrm{obs}} = V_{\mathrm{n}}^{\mathrm{obs}} \cos n\Psi_{\mathrm{n}}^{\mathrm{obs}} = \langle \cos n\varphi \rangle$$
$$V_{\mathrm{n,y}}^{\mathrm{obs}} = V_{\mathrm{n}}^{\mathrm{obs}} \sin n\Psi_{\mathrm{n}}^{\mathrm{obs}} = \langle \sin n\varphi \rangle\ .$$

Response function

$$p(V_{\mathrm{n}}^{\mathrm{obs}}|V_{\mathrm{n}}) \propto V_{\mathrm{n}}^{\mathrm{obs}} \exp\left[-\frac{(V_{\mathrm{n}}^{\mathrm{obs}})^2 + V_{\mathrm{n}}^2}{2\delta^2}\right] I_0\left(\frac{V_{\mathrm{n}}^{\mathrm{obs}} V_{\mathrm{n}}}{\delta^2}\right)$$

Unfolding matrix

$$M_{ij}^{\mathrm{iter}} = \frac{A_{ji} c_i^{\mathrm{iter}}}{\Sigma_{m,k} A_{mi} A_{jk} c_k^{\mathrm{iter}}},$$
$$\widehat{c}^{\mathrm{iter}+1} = \widehat{M}^{\mathrm{iter}} \widehat{e}, A_{ji} = p(e_j|c_i)$$

G.Aad et al. (ATLAS), JHEP 1311 (2013) 183

The method excludes the non-flow effects and extracts the genuine flow fluctuations

Fluctuations of elliptic flow in the model

Unsmeared parameter ε

Pb+Pb @ 2.76 ATeV

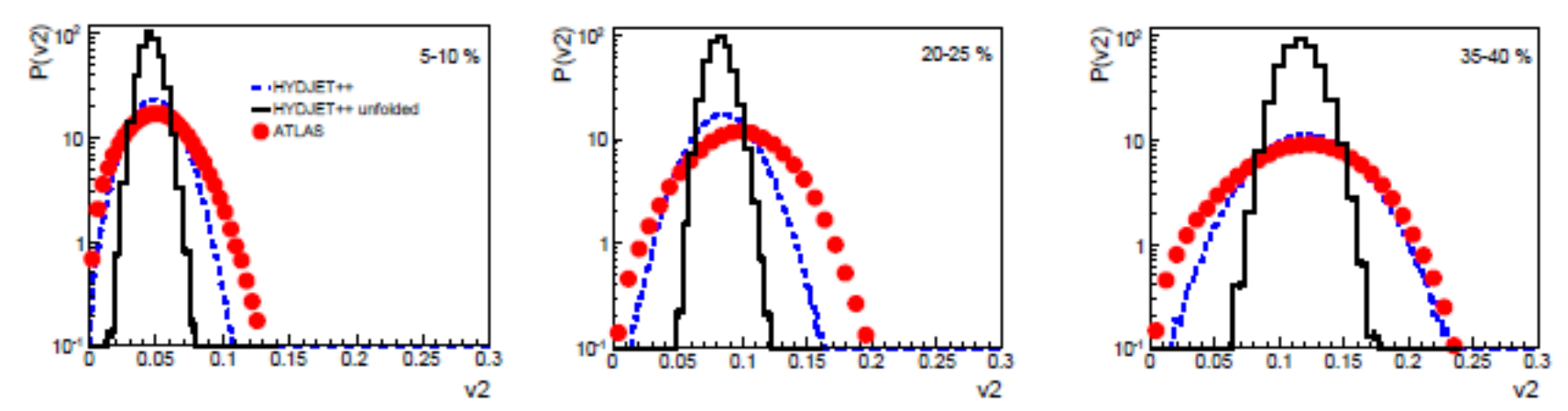

Normally smeared ε

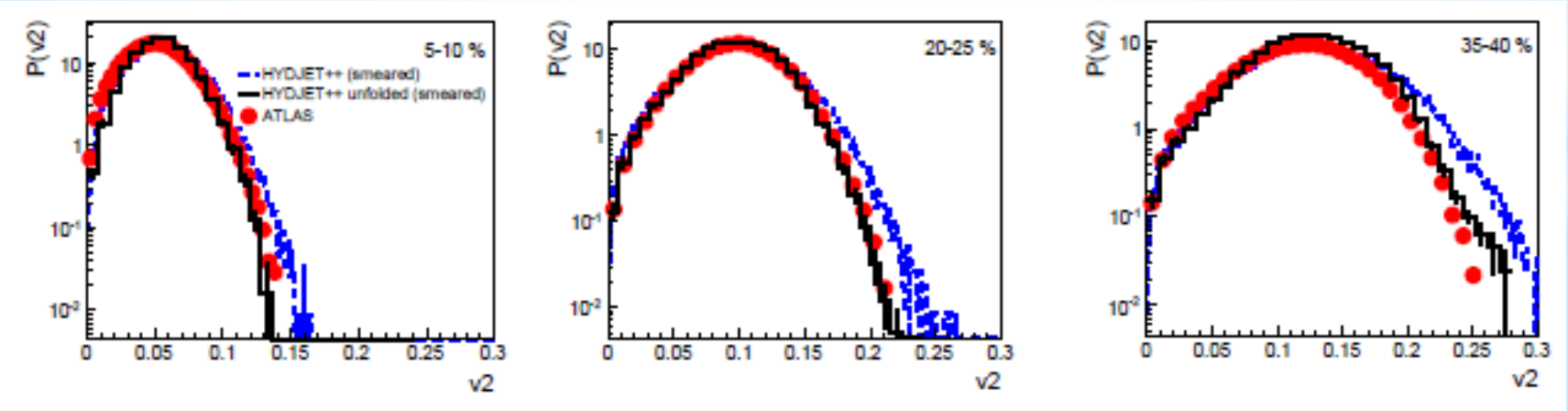

L.B. et al., to be submitted

Note: the smearing width for ε is optimized at one arbitrary centrality and then fixed for other centrality bins

Fluctuations of triangular flow in the model

Unsmeared parameter ε_3

Pb+Pb @ 2.76 ATeV

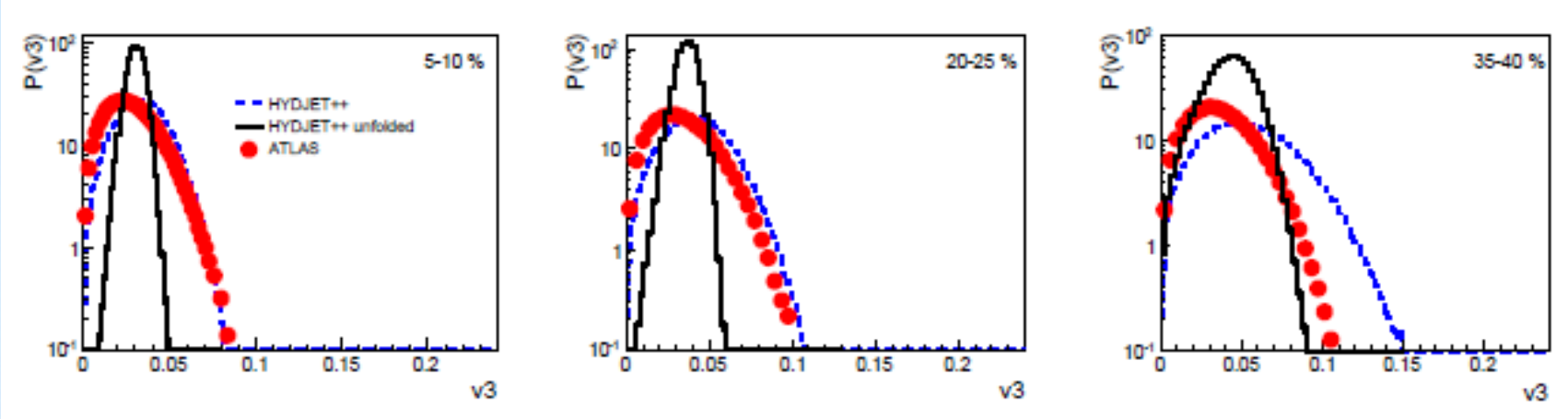

Normally smeared ε_3

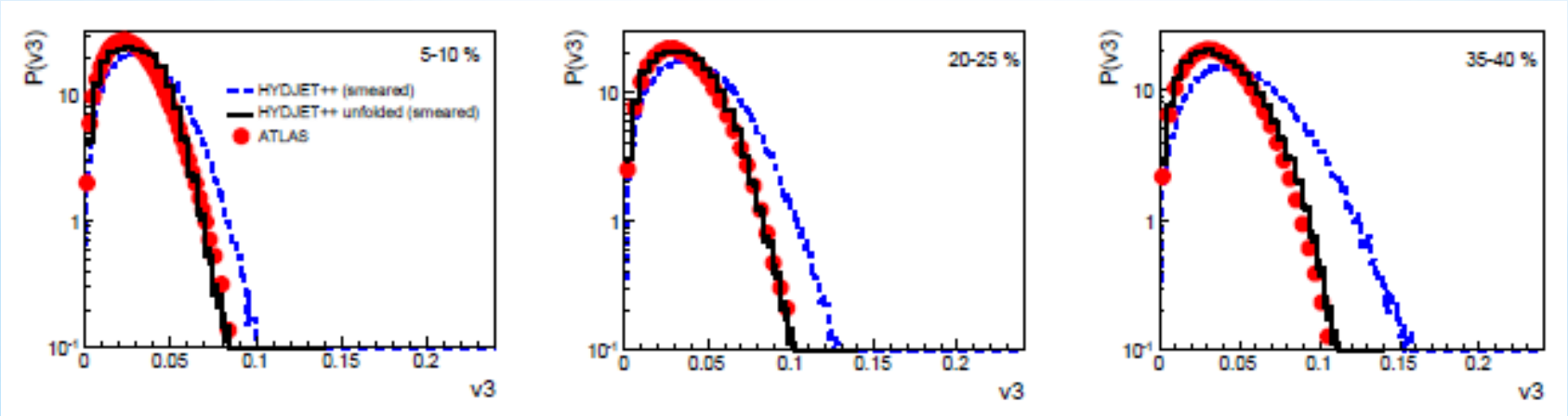

Note: the smearing width for ε_3 is optimized at one arbitrary centrality and then fixed for other centrality bins

CONCLUSIONS

The HYDJET++ model allows us to investigate flow of hydro and jet parts separately, to look at reconstruction of pure hydro flow and its modification due to jet part. It also enables to study cross-talk of v_2 and v_3, while other harmonics are absent.

1. ***Event-by-event distributions of anisotropic flow harmonics are studied in Pb+Pb collisions at LHC within the hydro-inspired freeze-out approach***
2. ***To compare model results with the data, unfolding procedure was employed. It removes also the non-flow fluctuations***
3. ***Dynamical origin of the flow fluctuations in the model: the fluctuations arise due to correlations between the (p_i,x_i) of the hadrons and the velocities of the fluid cells***
4. ***Gaussian smearing of two principal parameters permits to reproduce both elliptic and triangular flow fluctuations at LHC***

Back-up Slides

Relativistic heavy ion event generator HYDJET++

HYDJET++ (HYDrodynamics + JETs) - event generator to simulate heavy ion event by merging of two independent components (soft hydro-type part + hard multi-partonic state, the latter is based on PYQUEN - PYthia QUENched routine).

http://cern.ch/lokhtin/hydjet++ ***(latest version 2.1)***

[1] I. Lokhtin, L. Malinina, S. Petrushanko, A. Snigirev, I. Arsene, K. Tywoniuk, Comp. Phys. Comm. 180 (2009) 77

[2] I. Lokhtin, A. Belyaev, L. Malinina, S. Petrushanko, E. Rogochaya, A. Snigirev, Eur. Phys. J. C 72 (2012) 2045

[3] L. Bravina, H. Brusheim Johansson, G. Eyyubova, V. Korotkikh, I. Lokhtin, L. Malinina, S. Petrushanko, A. Snigirev, E. Zabrodin, Eur. Phys. J. C 74 (2014) 2807

HYDJET++ (soft): main physics assumptions

A hydrodynamic expansion of the fireball is supposed to end by a sudden system breakup at given T and chemical potentials. Momentum distribution of produced hadrons keeps the thermal character of the equilibrium distribution.

Cooper-Frye formula:

$$p^0 \frac{d^3 N_i}{d^3 p} = \int_{\sigma(x)} d^3\sigma_\mu(x) p^\mu f_i^{eq}(p^\nu u_\mu(x); T, \mu_i)$$

- HYDJET++ avoids straightforward 6-dimensional integration by using the special simulation procedure (like HYDJET): momentum generation in the rest frame of fluid element, then Lorentz transformation in the global frame → uniform weights → effective von-Neumann rejection-acception procedure.

Freeze-out surface parameterizations

1. The Bjorken model with hypersurface $\tau = (t^2 - z^2)^{1/2} = const$
2. Linear transverse flow rapidity profile $\rho_u = \frac{r}{R}\rho_u^{\max}$
3. The total effective volume for particle production at

- $$V_{eff} = \int_{\sigma(x)} d^3\sigma_\mu(x) u^\mu(x) = \tau \int_0^R \gamma_r r dr \int_0^{2\pi} d\phi \int_{\eta_{\min}}^{\eta_{\max}} d\eta = 2\pi\tau\Delta\eta \left(\frac{R}{\rho_u^{\max}}\right)^2 (\rho_u^{\max}\sinh\rho_u^{\max} - \cosh\rho_u^{\max} + 1)$$

HYDJET++ (soft): hadron multiplicities

1. The hadronic matter created in heavy-ion collisions is considered as a hydrodynamically expanding fireball with EOS of an ideal hadron gas.

$$N_i = \rho_i(T, \mu_i) V_{eff}$$

2. "Concept of effective volume" T=const and μ=const: the total yield of particle species is

$$T(\mu_B) = a - b\mu_B - c\mu_B^4; \mu_B(\sqrt{s_{NN}}) = \frac{d}{1 + e\sqrt{s_{NN}}}$$

3. Chemical freeze-out : T, $\mu_i = \mu_B B_i + \mu_S S_i + \mu_c C_i + \mu_Q Q_i$; T, μ_B –can be fixed by particle ratios, or by phenomenological formulas

$$f_i^{eq}(p^{0*}; T, \mu_i) = \frac{1}{(2\pi)^3} \frac{g_i}{\exp([p^{0*} - \mu_i]/T) \pm 1}$$

4. Chemical freeze-out: all macroscopic characteristics of particle system are determined via a set of equilibrium distribution functions in the fluid element rest frame:

$$\rho_i^{eq}(T, \mu_i) = \int_0^\infty d^3\vec{p}^{\,*} f_i^{eq}(p^{0*}; T(x^*), \mu(x^*)_i) = 4\pi \int_0^\infty dp^* p^{*2} f_i^{eq}(p^{0*}; T, \mu_i)$$

HYDJET++ (soft): thermal and chemical freeze-outs

1. The particle densities at the chemical freeze-out stage are too high to consider particles as free streaming and to associate this stage with the thermal freeze-out

2. Within the concept of chemically frozen evolution, the conservation of the particle number ratios from the chemical to thermal freeze-out is assumed:

$$\frac{\rho_i^{eq}(T^{ch},\mu_i^{ch})}{\rho_\pi^{eq}(T^{ch},\mu_\pi^{ch})} = \frac{\rho_i^{eq}(T^{th},\mu_i^{th})}{\rho_\pi^{eq}(T^{th},\mu_\pi^{th})}$$

3. The absolute values of $\rho_i^{eq}(T^{th},\mu_i^{th})$ are determined by the choice of the free parameter of the model: effective pion chemical potential $\mu_\pi^{eff,th}$ at T^{th}
For hadrons heavier than pions the Boltzmann approximation is assumed:

$$\mu_i^{th} = T^{th}\ln\left(\frac{\rho_i^{eq}(T^{ch},\mu_i^{ch})}{\rho_i^{eq}(T^{th},\mu_i=0)}\,\frac{\rho_\pi^{eq}(T^{th},\mu_\pi^{eff,th})}{\rho_\pi^{eq}(T^{ch},\mu_i^{ch})}\right)$$

Particle momentum spectra are generated on the thermal freeze-out hypersurface, the hadronic composition at this stage is defined by the parameters of the system at chemical freeze-out

HYDJET++ (soft): input parameters

1-5. Thermodynamic parameters at chemical freeze-out: T_{ch} , $\{\mu_B, \mu_S, \mu_C, \mu_Q\}$ (option to calculate T_{ch}, μ_B and μ_s using phenomenological parameterization $\mu_B(\sqrt{s})$, $T_{ch}(\mu_B)$ is foreseen).

6-7. Strangeness suppression factor $\gamma_S \leq 1$ and charm enchancement factor $\gamma_c \geq 1$ (options to use phenomenological parameterization $\gamma_S(T_{ch}, \mu_B)$ and to calculate γ_c are foreseen).

8-9. Thermodynamical parameters at thermal freeze-out: T_{th} , and μ_π- effective chemical potential of positively charged pions.

10-12. Volume parameters at thermal freeze-out: proper time τ_f , its standard Deviation (emission duration) $\Delta\tau_f$, maximal transverse radius R_f .

13. Maximal transverse flow rapidity at thermal freeze-out ρ_{umax} .

14. Maximal longitudinal flow rapidity at thermal freeze-out η_{max} .

15. Flow anisotropy parameter: $\delta(b) \rightarrow u_\mu = u_\mu(\delta(b),\varphi)$

16. Coordinate anisotropy:

$$\varepsilon(b) \rightarrow R_f(b)=R_f(0)[V_{eff}(\varepsilon(0),\delta(0))/V_{eff}(\varepsilon(b),\delta(b))]^{1/2}[N_{part}(b)/N_{part}(0)]^{1/3}$$

For impact parameter range bmin-bmax:

$$V_{eff}(b)=V_{eff}(0)N_{part}(b)/N_{part}(0), \quad \tau_f(b)=\tau_f(0)[N_{part}(b)/N_{part}(0)]^{1/3}$$

Freeze-out hypersurface for non-central collisions

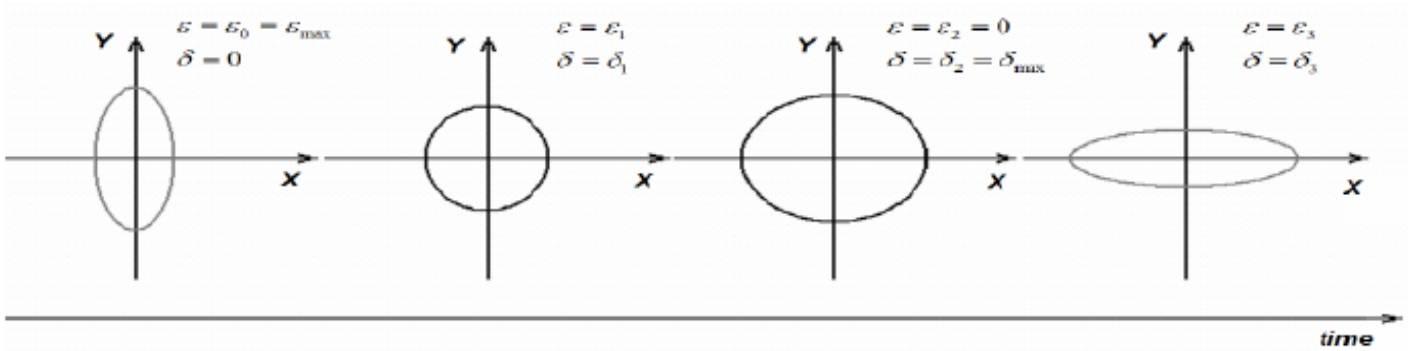

In non-central collisions the shape of the emission region is approximated by an ellipse

$$R(b,\phi)=R_s(b)\frac{\sqrt{1-\epsilon^2(b)}}{\sqrt{1+\epsilon(b)\cos(2\phi)}}$$ the freezeout fireball radius in the reaction plane

$\epsilon(b)$ ellipse eccentricity in the z-x plane

$$R_s(b)=\sqrt{(R_x^2+R_y^2)/2}$$

We use a scaling approximation Lokhtin and Snigirev, Eur.Phys.J. C45, 211 (2006)

$R_s(b)=R_s(b=0)\sqrt{1-\epsilon_s(b)}$ where $R_s(b=0)=R$ is the fireball radius in central collisions

$\epsilon_s(b)$ is used as an input parameter which depends on collision energy, radius of colliding nuclei and impact parameter.

Momenta anisotropy

Since we do not trace the hydro evolution, we have to introduce also a parameter for the momenta anysotropy developed during the hydro evolution.

The azimuthal angle of the fluid velocity vector is rotated so that is not identical with the spatial azimuthal angle.

$$u^{\mu}(t,\vec{x})=\{\gamma_{\phi}\cosh\rho_{u}\cosh\eta_{u},\sqrt{1+\delta(b)}\sinh\rho_{u}\cos\phi,\sqrt{1-\delta(b)\sinh\rho_{u}}\sin\phi,\gamma_{\phi}\cosh\rho_{u}\sinh\eta_{u}\}$$

where $\gamma_{\phi}=\sqrt{1+\delta(b)\tanh^{2}\rho_{u}\cos(2\phi)}$

The fluid velocity azimuthal angle is related to the spatial azimuthal angle trough:

$$\tan\phi_{u}=\sqrt{\frac{1-\delta(b)}{1+\delta(b)}}\tan\phi$$

Monte-Carlo simulation of hard component (including nuclear shadowing) in HYDJET/HYDJET++

- Calculating the number of hard NN sub-collisions Njet (b, Ptmin, $\sqrt{s}$) with Pt>Ptmin around its mean value according to the binomial distribution.
- Selecting the type (for each of Njet) of hard NN sub-collisions (pp, np or nn) depending on number of protons (Z) and neutrons (A-Z) in nucleus A according to the formula: $Z=A/(1.98+0.015A^{2/3})$.
- Generating the hard component by calling PYQUEN njet times.
- Correcting the PDF in nucleus by the accepting/rejecting procedure for each of Njet hard NN sub-collisions: comparision of random number generated uniformly in the interval [0,1] with shadowing factor S(r1,r2,x1,x2,Q2) ≤ 1 taken from the adapted impact parameter dependent parameterization based on Glauber-Gribov theory (*K.Tywoniuk et al., Phys. Lett. B 657 (2007) 170*).

Ratio v_3^2/v_2^3 for different production modes

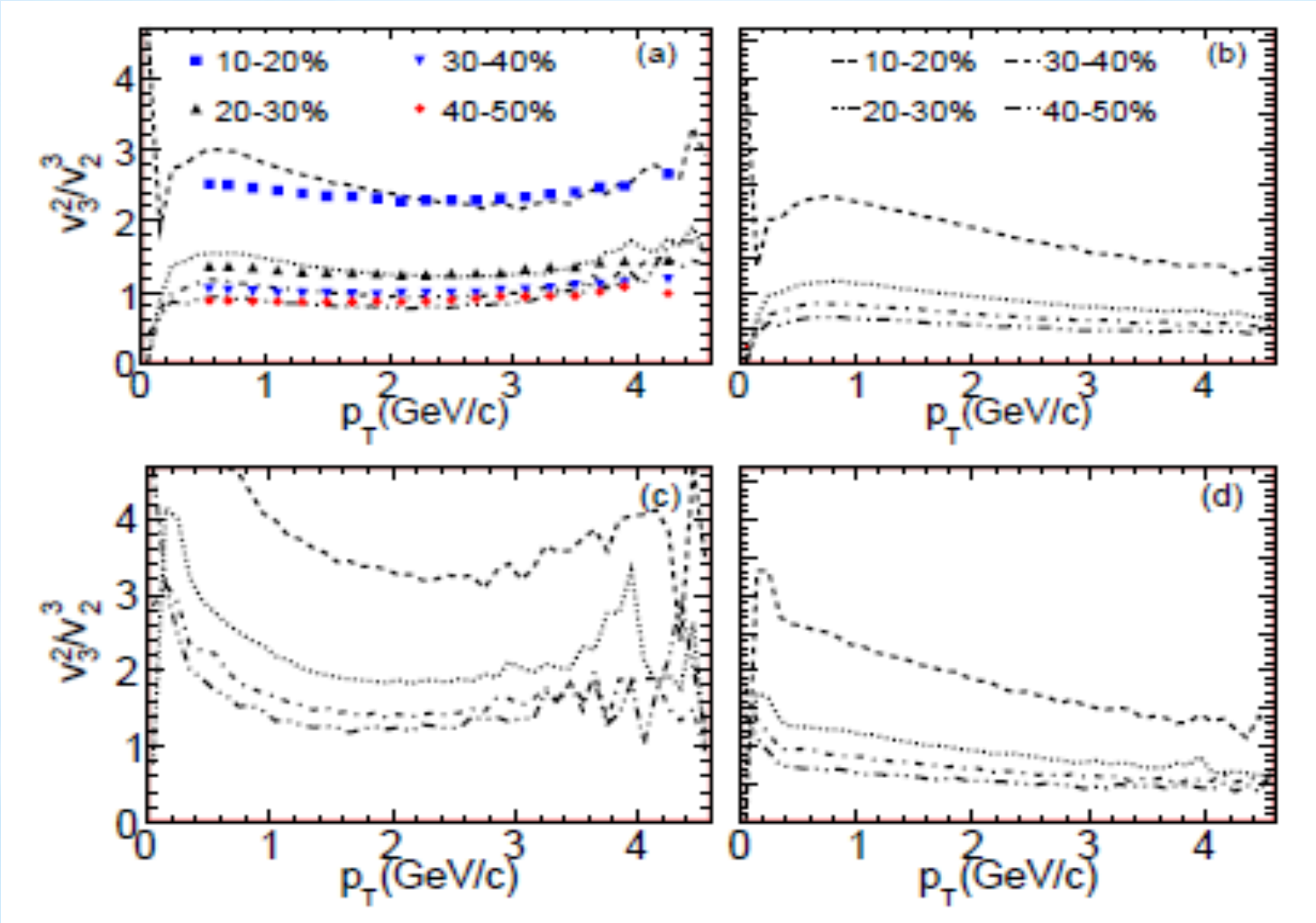

B.H. Brusheim Johansson et al., to be submitted

(a) all ; (b) hydro + decays ; (c) directly produced ; (d) hydro w/o decays

The pT specta of π, K, p, Λ with HYDJET++ model (RHIC)

The slope for the hydro part depends strongly on mass:

- the heavier the particle -- the harder the spectrum

The hydro part dies out earlier for light particles than for heavy ones

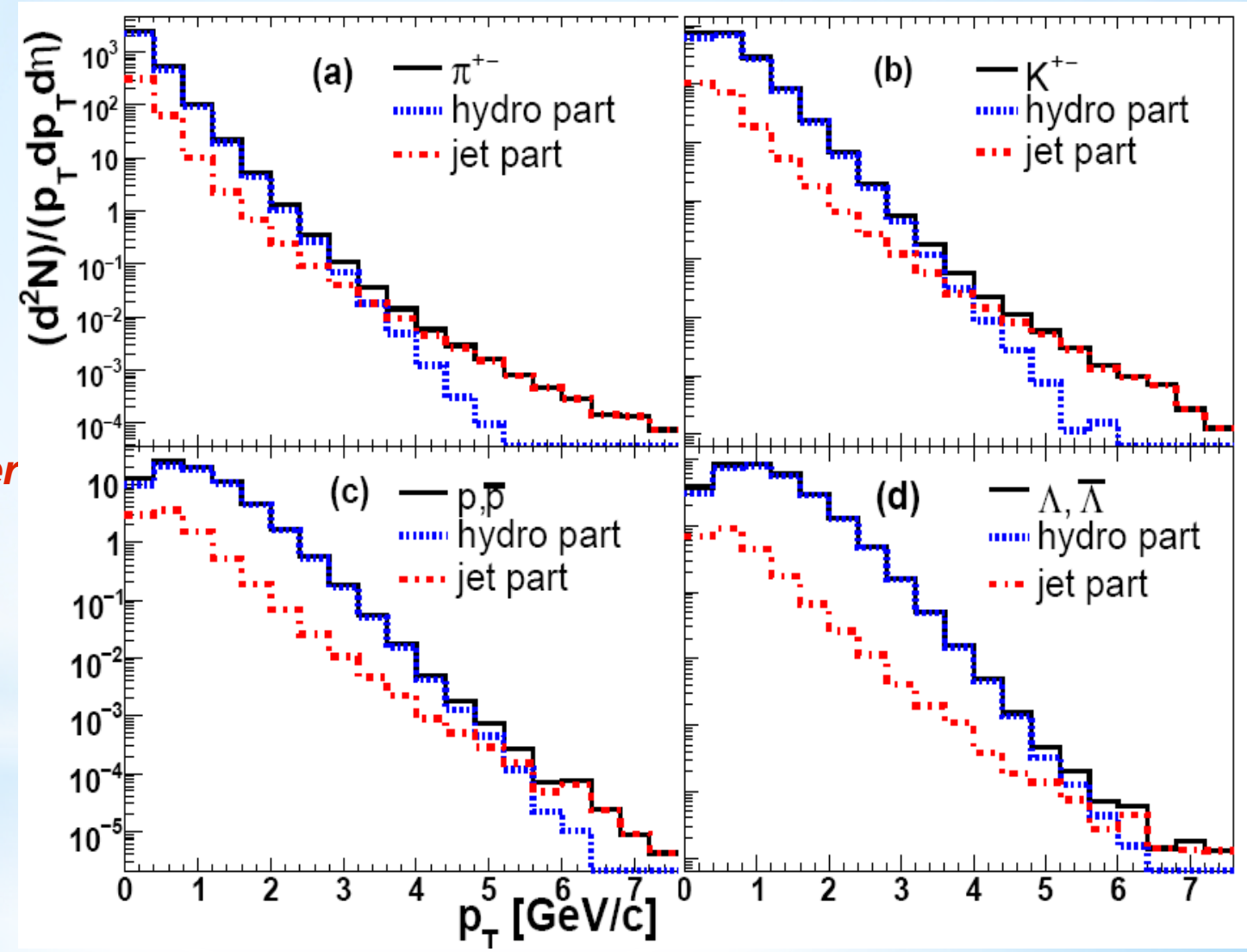

Transverse momentum of secondary particles

$\Delta \rightarrow \pi + p$

	$\pi^{\pm}$	$K + \bar{K}$	$p + \bar{p}$	$\Lambda + \bar{\Lambda} + \Sigma + \bar{\Sigma}$	ϕ
all	860	185	63.8	42.3	6.55
direct	169	81.4	18.6	14.2	6.5
direct %	20 %	44 %	30 %	39 %	99 %

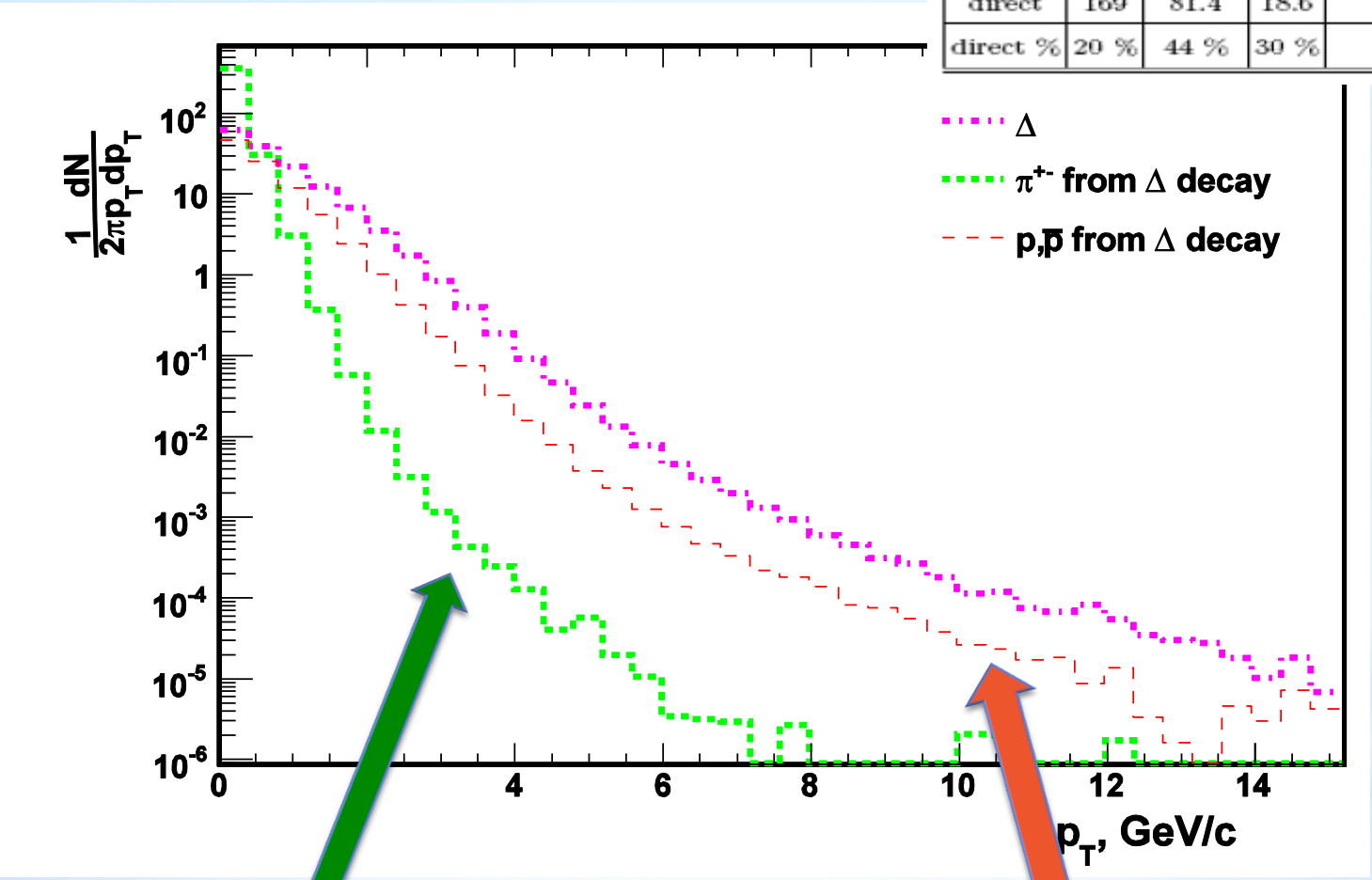

The secondary pion spectrum is much softer than proton spectrum

IV . Influence of resonance decays

Influence of resonance decays on v3 of different particles at LHC

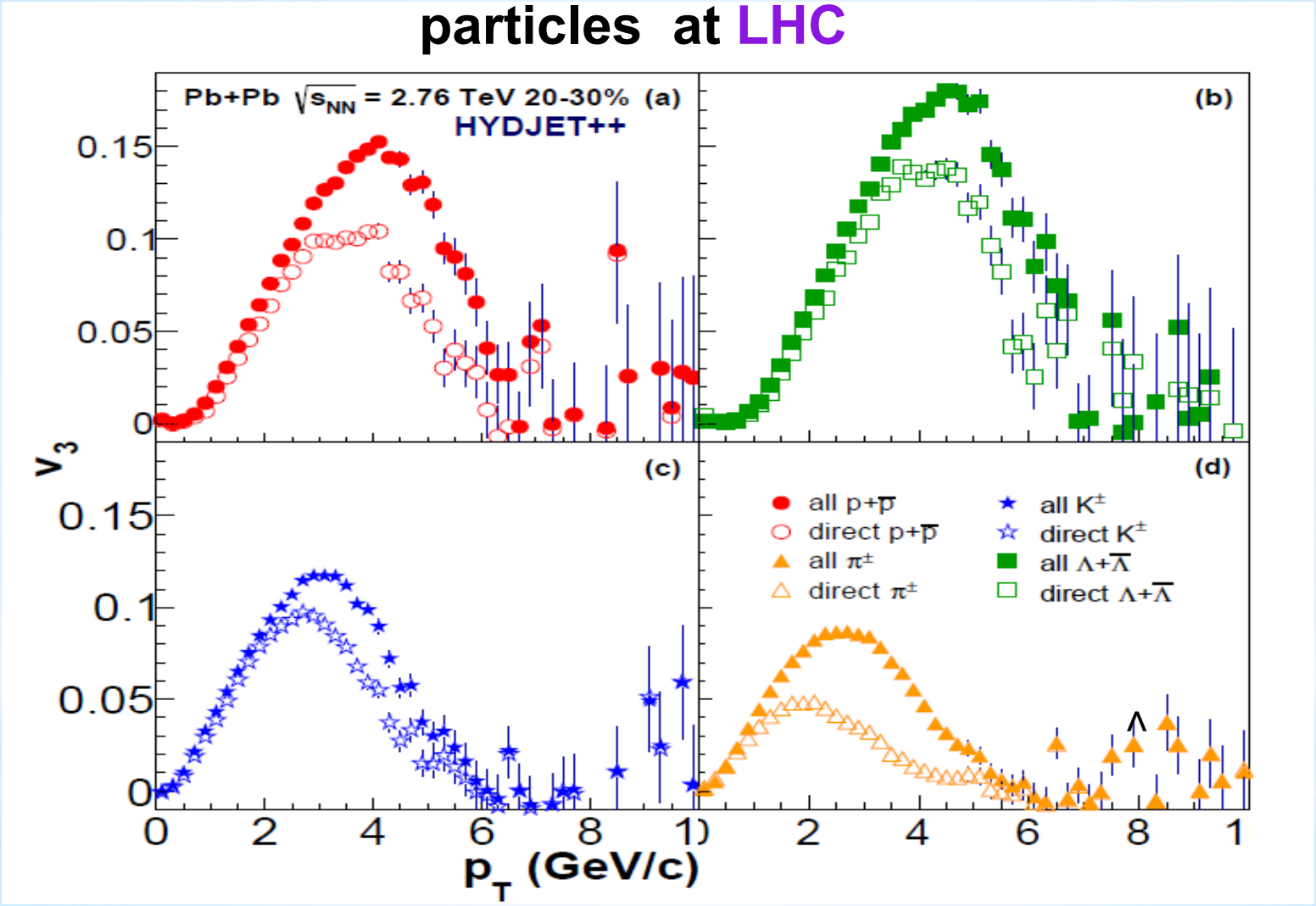

J. Crkovska et al., to be submitted

Pions, Kaons, Baryons: the maximum of the resulting flow is shifted to higher pT compared to the flow of directly produced particles

Triangular flow of direct and secondary particles at LHC

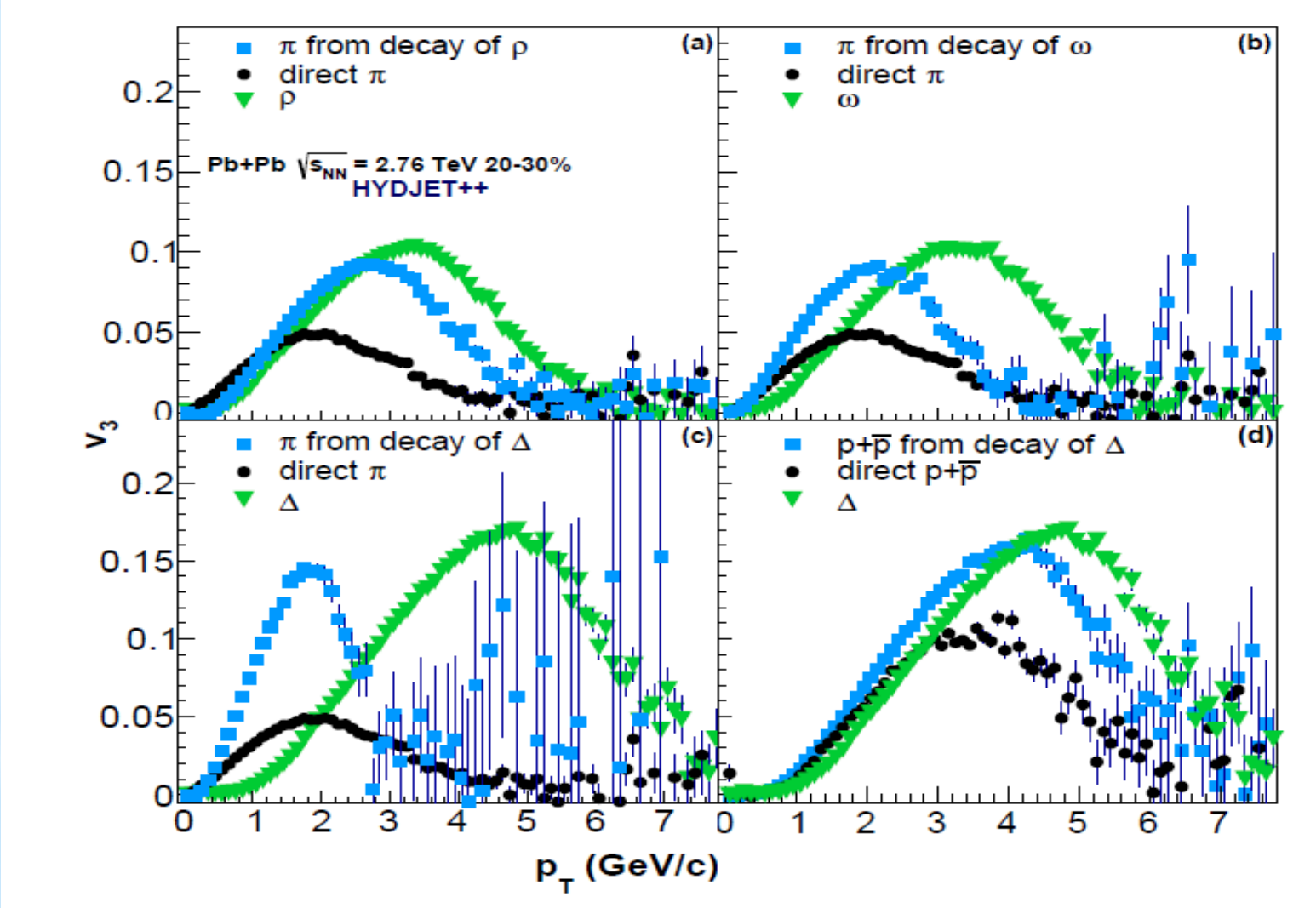

J. Crkovska et al., to be submitted

(Similar to elliptic flow): At low transverse momenta pions from baryon resonances enhance the flow whereas pions from meson resonances reduce it

LHC data vs. HYDJET++ model

Pb+Pb @ 2.76 ATeV

Transverse momentum

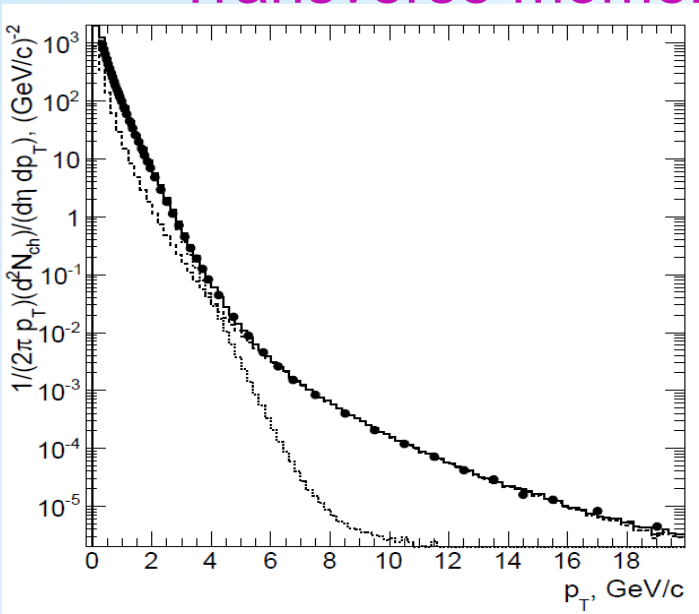

Rapidity

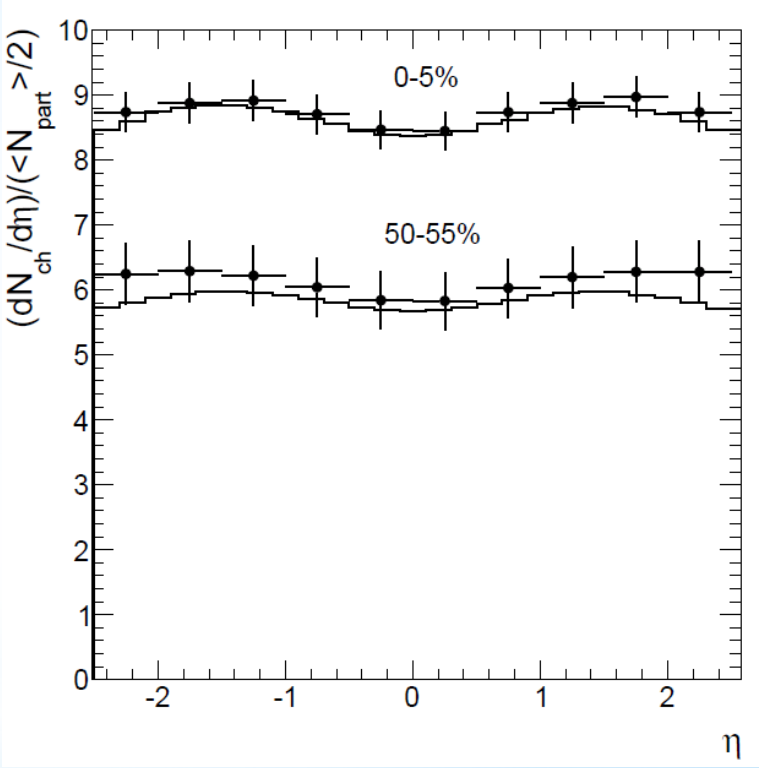

I. Lokhtin et al., Eur. Phys. J C72 (2012) 2045

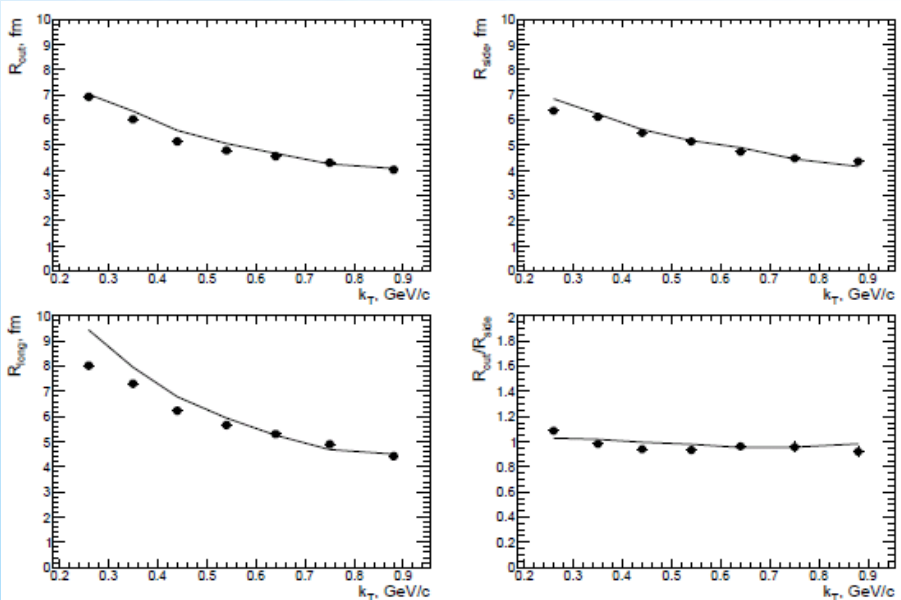

Correlation radii (femtoscopy)

V. Number-of-constituent-quark (NCQ) scaling

Number-of-constituent-quark scaling at RHIC

Direct particles: scaling is not good. All particles: KET/nq scaling

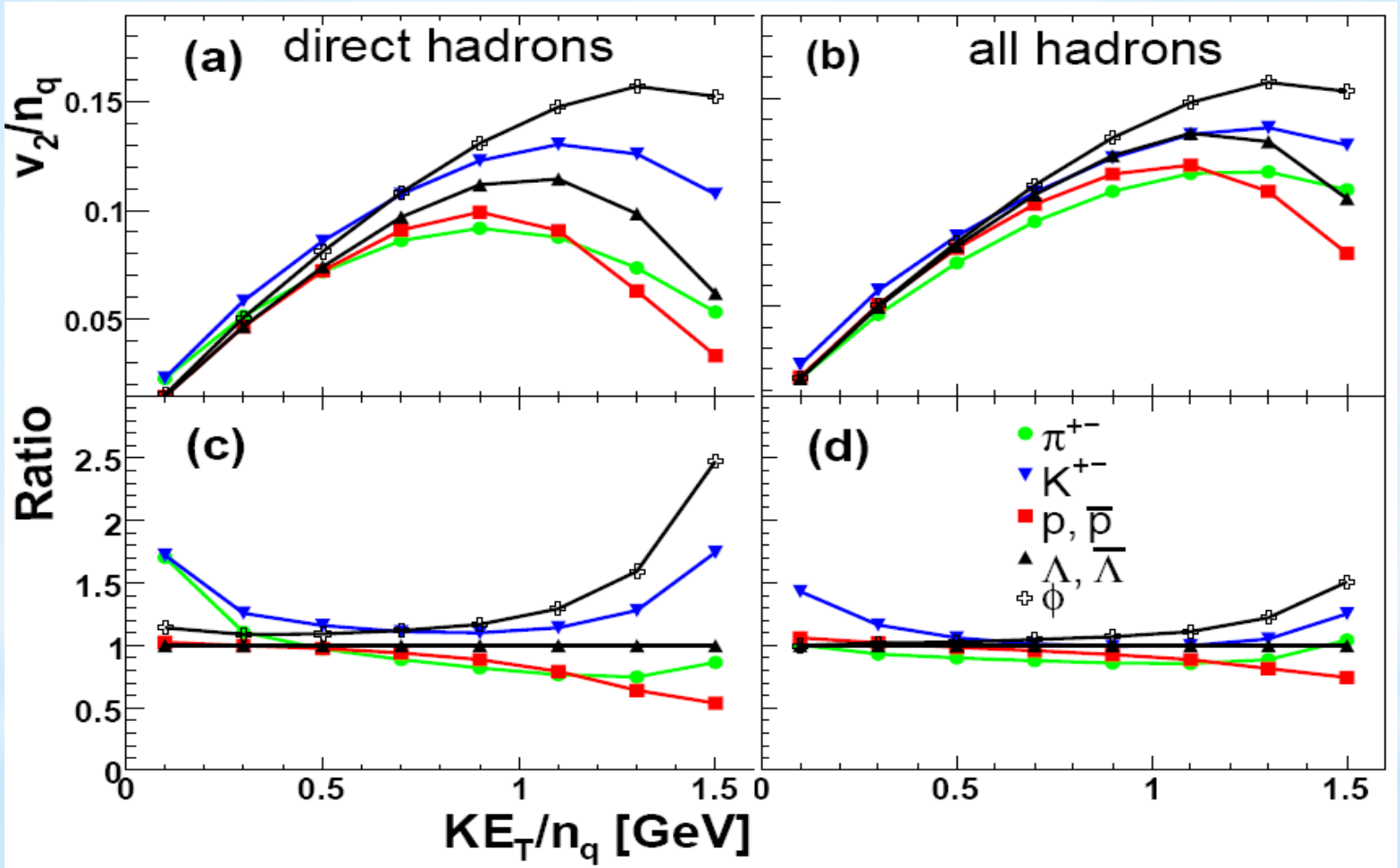

G.Eyyubova et al., PRC 80 (2009) 064907

One of the explanations of KET/nq scaling is partonic origin of the elliptic flow.

However, final state effects (such as resonance decays and jets) may also lead to appearance of the scaling

NCQ scaling for v2 at LHC

No scaling for direct particles

Appearance of the approximate scaling for all particles

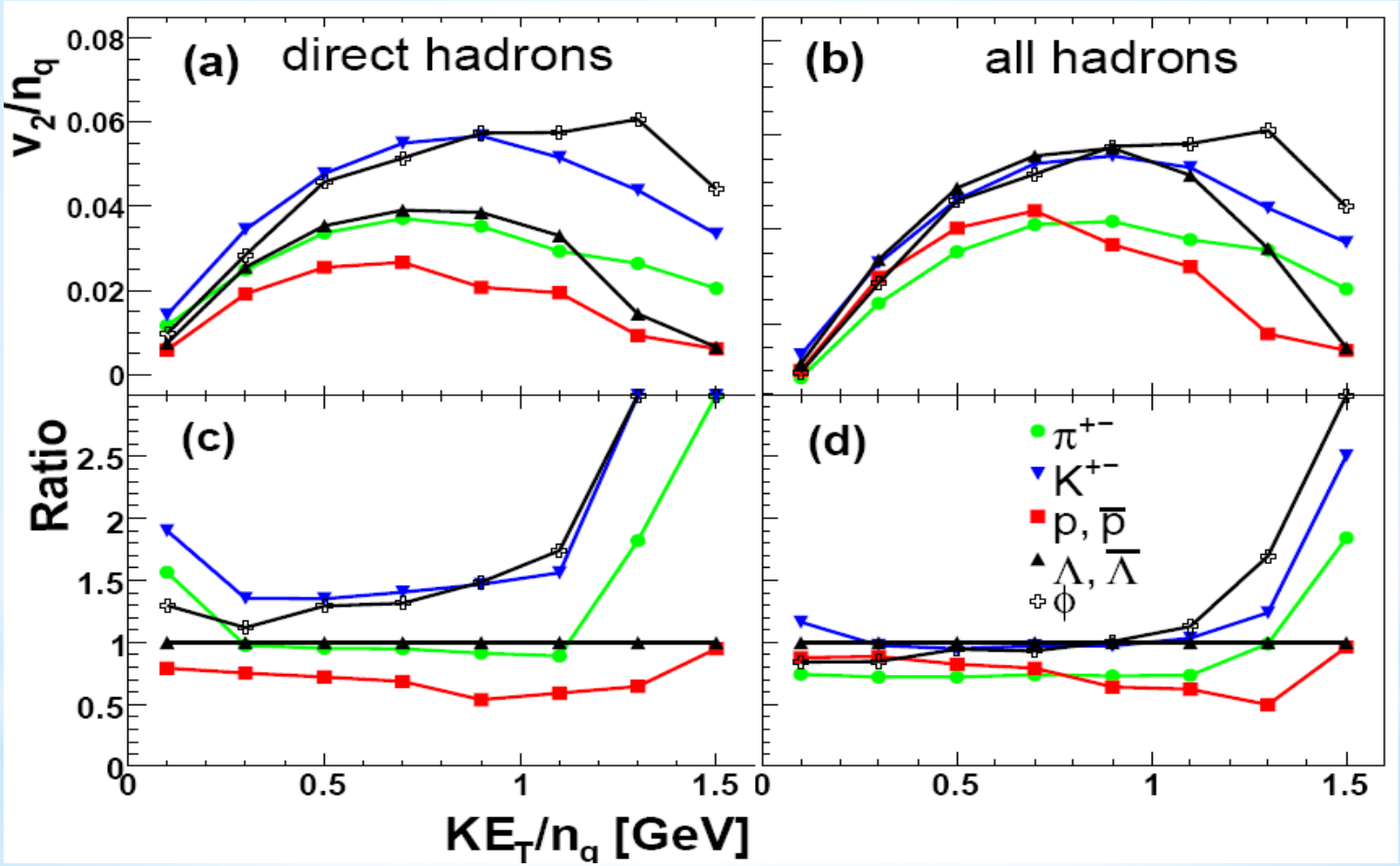

G.Eyyubova et al., PRC 80 (2009) 064907

LHC: NCQ scaling will be only approximate (prediction, 2009)

Experimental results (LHC)

ALICE Collaboration, M. Krzewicki et al., JPG 38 (2011) 124047

Semi-sentral collisions

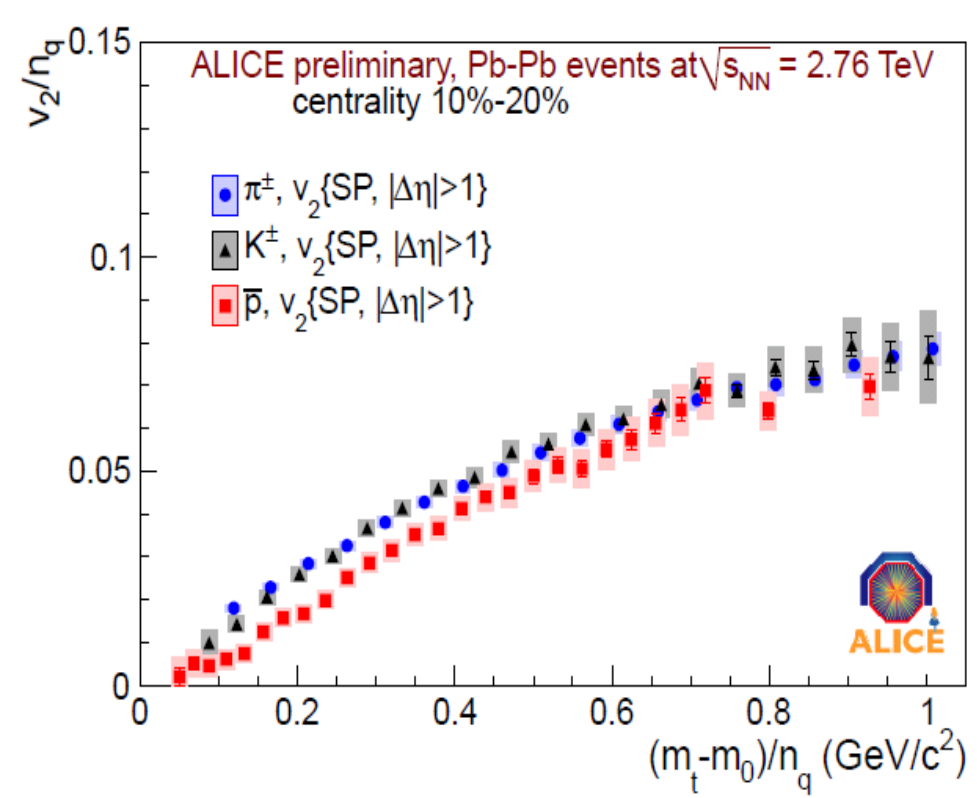

Semi-peripheral collisions

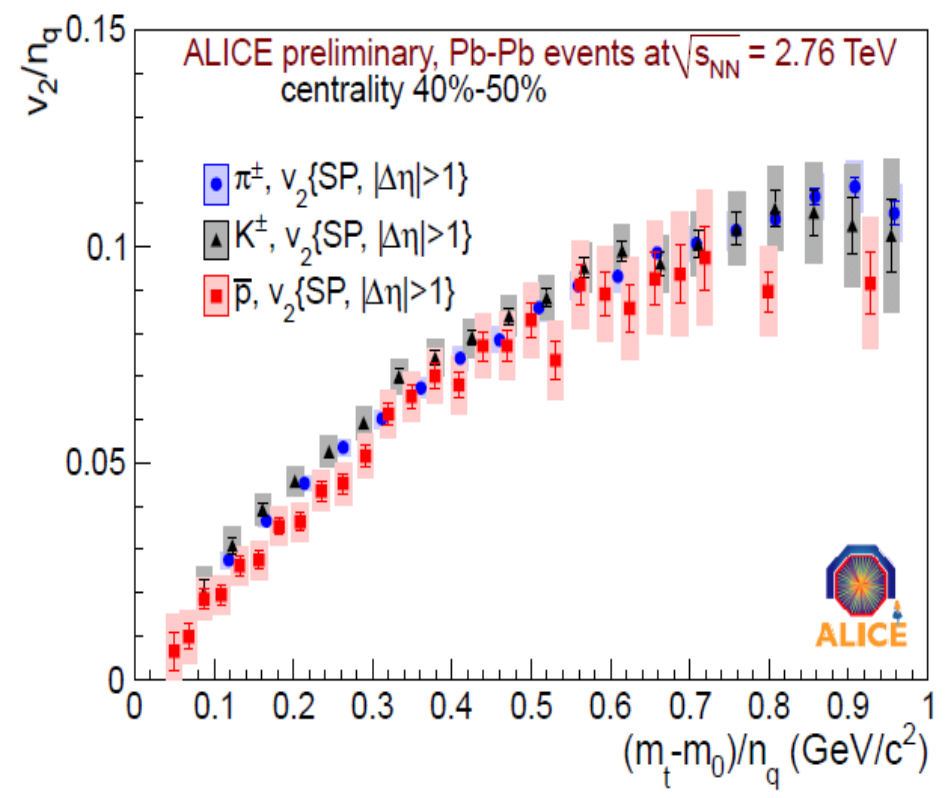

The NCQ scaling is indeed only approximate (2011)

NCQ-scaling of elliptic flow at beam energy scan (RHIC)

STAR Collab., PRL 110 (2013) 142301

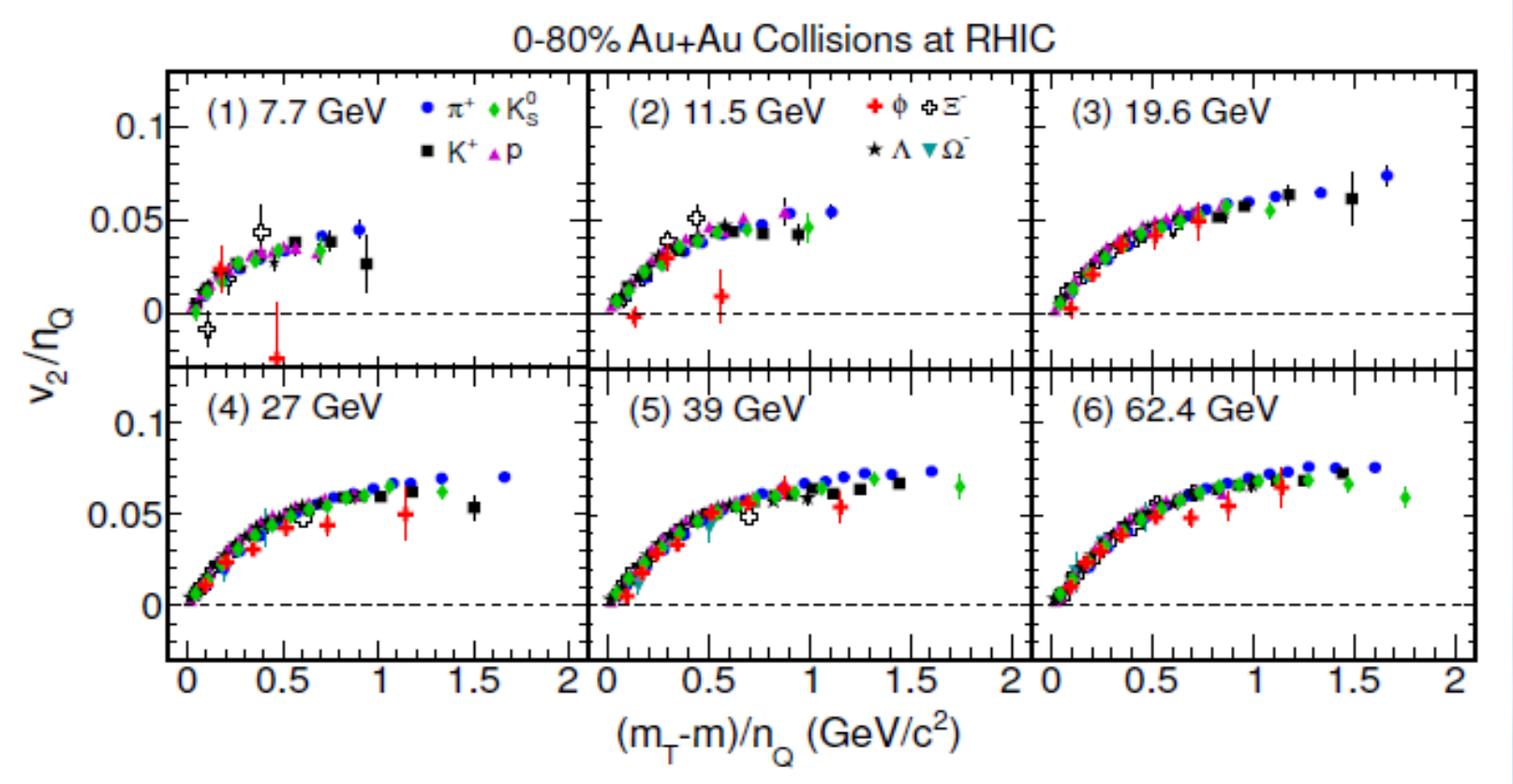

- NCQ scaling holds for particles and anti-particles separately at lower energies

Our explanation: jets (more influental at higher energies) violate the NCQ-scaling, whereas Hydro+Resonances work towards its fulfilment

NCQ scaling for v3 at LHC

No scaling for direct particles

After resonance decays

Approximate scaling for all particles

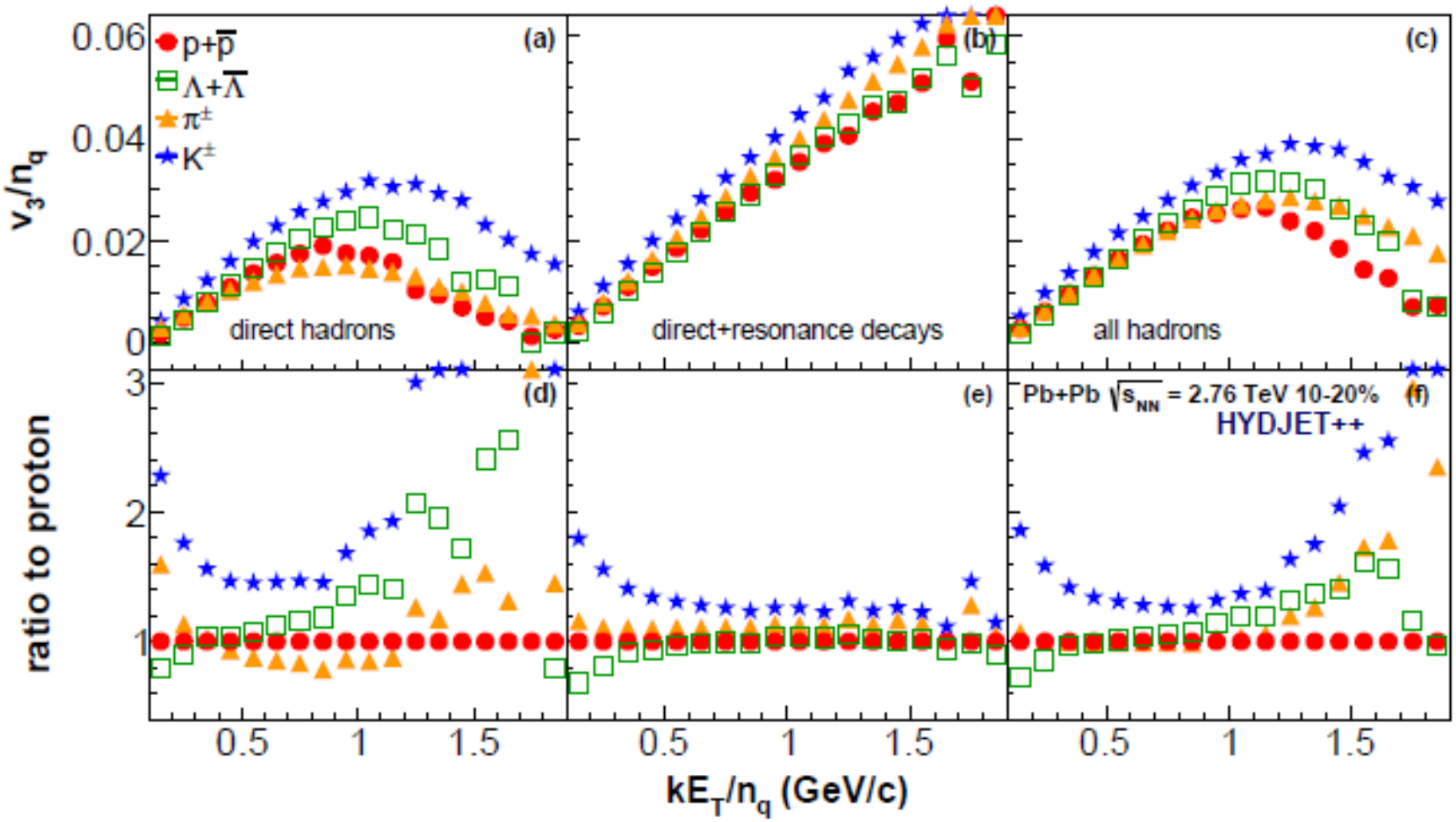

J. Crkovska et al., to be submitted.

NCQ scaling for triangular flow is similar to that for the elliptic flow

VI. Interplay of v2 and v3

Hexagonal flow: $V_6 \propto \alpha V_2^3 + \beta V_3^2$

Bravina et al., PRC 89, 024909 (2014)

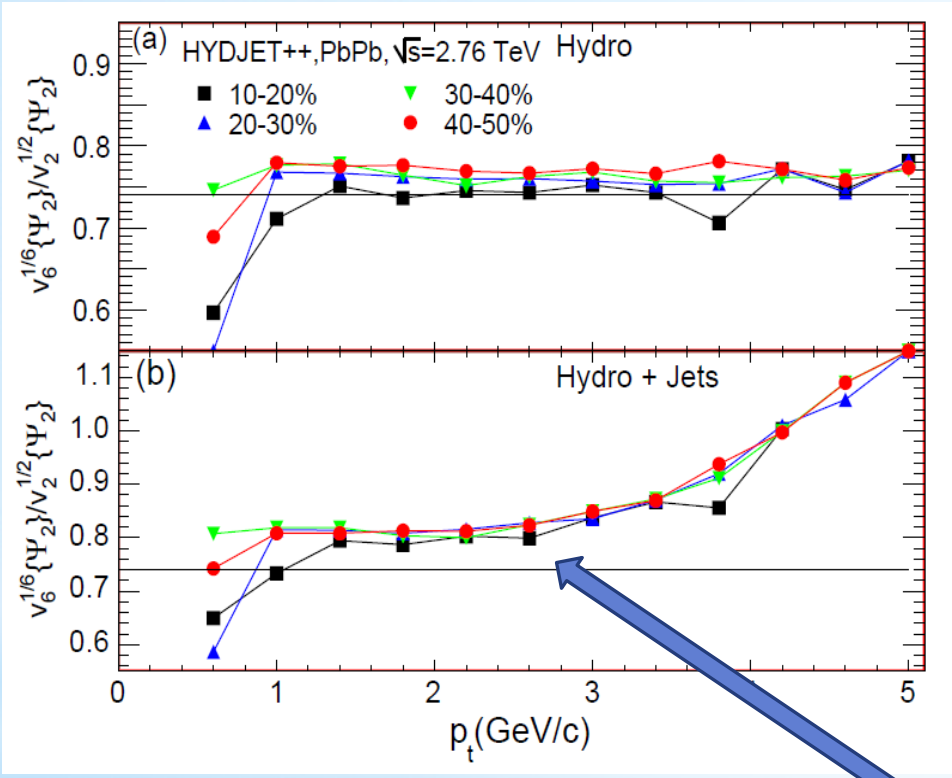

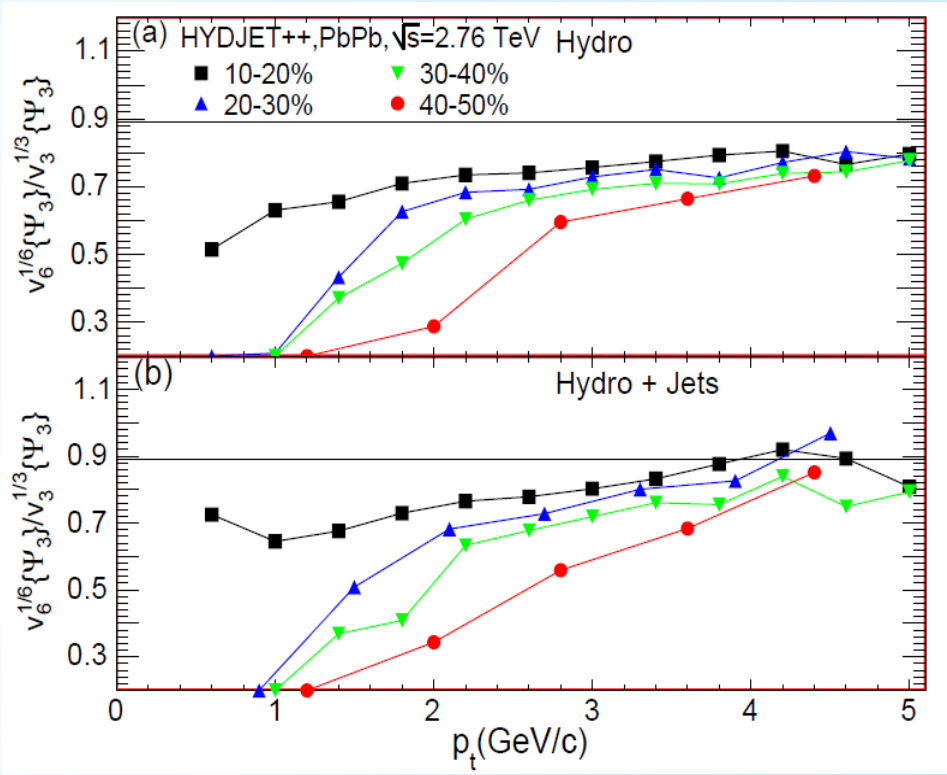

Ψ_2 Scaling? Ψ_3

It would be interesting to study $V_6(\Psi_2)$ and $V_6(\Psi_3)$ in experiment

Hexagonal flow: centrality dependence

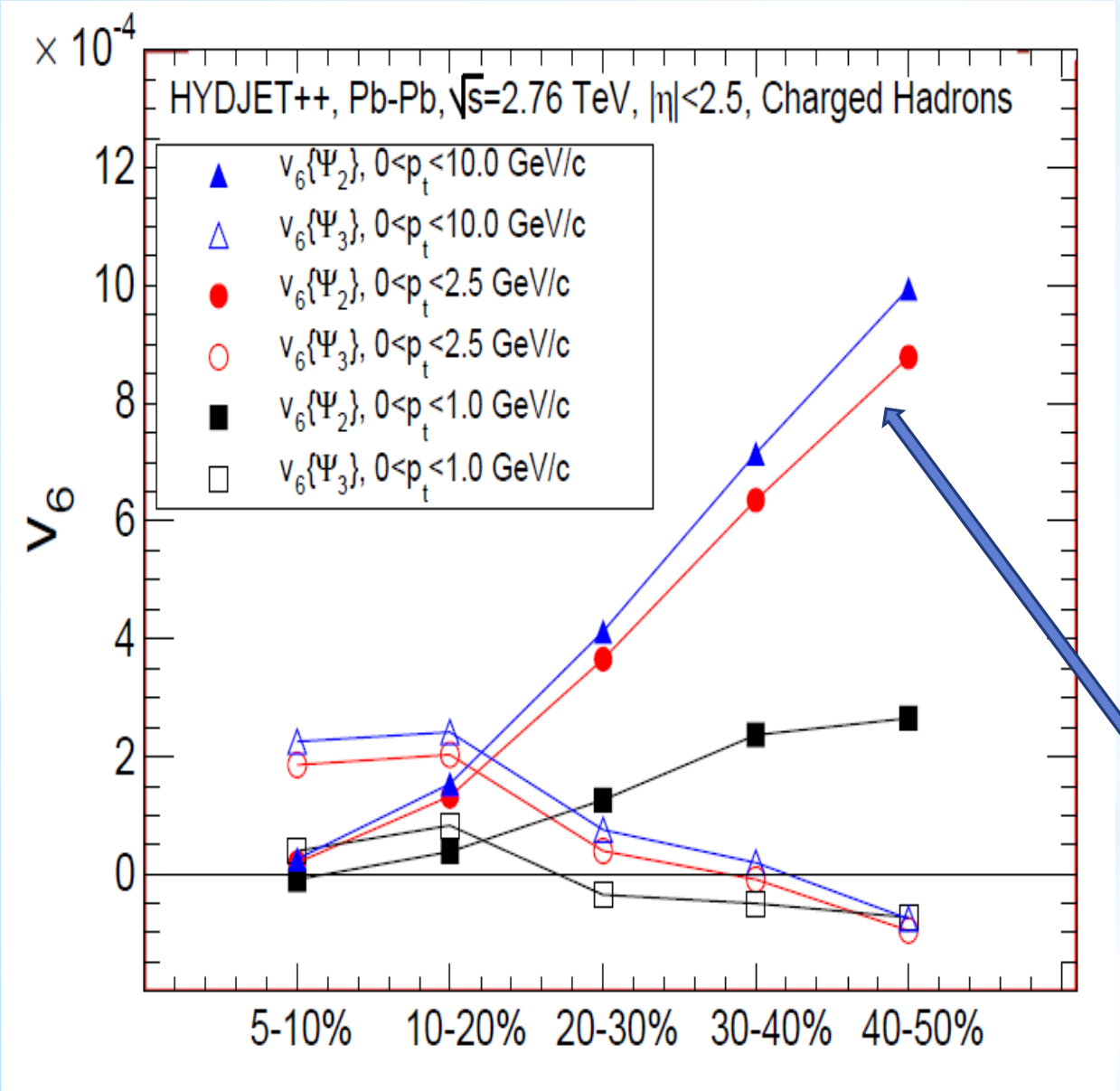

CMS Collab., PRC 89, 024909 (2014)

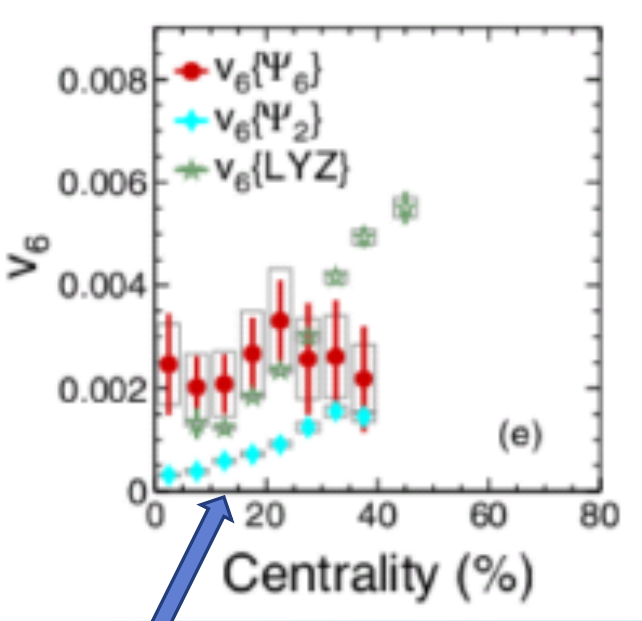

Centrality dependence in HYDJET++ is correct

Methods for **v2** calculation

(1) Event plane method

$$v_2^{obs}\{EP\} = \langle \cos 2(\varphi_i - \Psi_2) \rangle$$

Ψ2 is the calculated reaction plane angle: $\tan n\psi_n = \dfrac{\sum_i \omega_i \sin n\varphi_i}{\sum_i \omega_i \cos n\varphi_i}, \quad n \geq 1, \quad 0 \leq \psi_n < 2\pi / n$

$$v_2\{EP\} = \frac{v_2^{obs}\{EP\}}{R} = \frac{v_2^{obs}\{EP\}}{\langle \cos 2(\Psi_2 - \Psi_R) \rangle}$$

(2) Two particle correlation method $v_2\{2\} = \sqrt{\langle \cos 2(\varphi_i - \varphi_j) \rangle}$

(3) Lee-Yang zero method $G(ir) = \langle e^{irQ} \rangle, Q = \sum \cos(2\varphi)$

Integral v2 is connected with the firs minimum r0 of the module of the G(ir):

$$v_2 = \frac{j_0}{N r_0}$$

Differential flow is calculated by the formula: $\dfrac{v_2(p_T)}{N v_2} = \mathrm{Re}\left(\dfrac{\langle \cos(2\varphi) e^{ir_0 Q} \rangle}{\langle Q e^{ir_0 Q} \rangle} \right)$

Comparison of Event Plane and Lee-Yang zeroes methods (c=30%)

EventPlane method

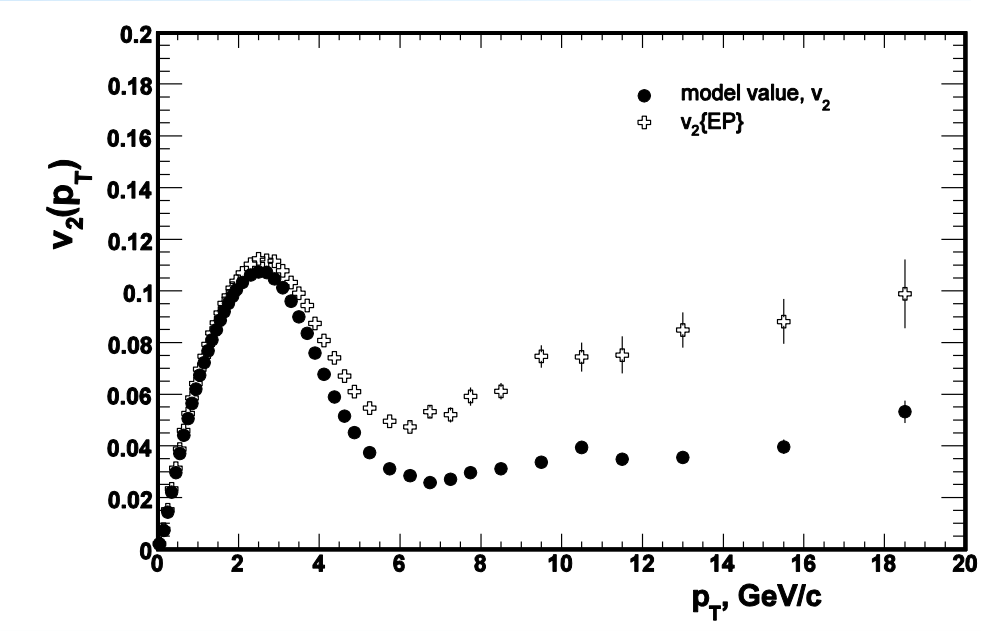

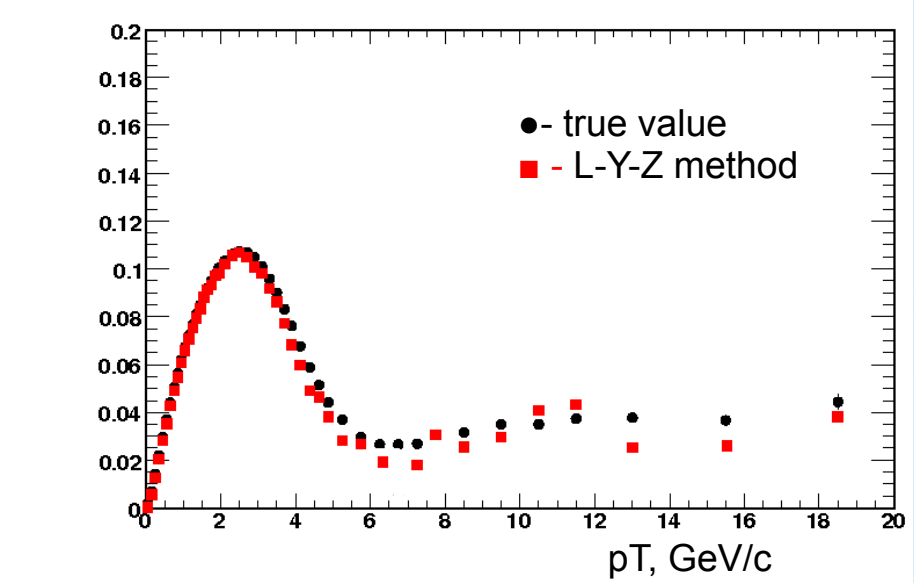

Lee-Yang zeroes Method

Event Plane method overestimates v2 at high pt due to non-flow correlation (mostly because of jets).